AD_____

Award Number: **W81XWH-08-1-0783**

TITLE: **Generation of soluble Receptor Activator of NF-kappa B Ligand is critical for osteolytic Bone Metastasis**

PRINCIPAL INVESTIGATOR: **Kalyan C. Nannuru**

CONTRACTING ORGANIZATION:

University of Nebraska Medical Center

Omaha, NE 68198-5900

REPORT DATE: **October 2009**

TYPE OF REPORT: **Annual Summary**

PREPARED FOR: U.S. Army Medical Research and Materiel Command
Fort Detrick, Maryland 21702-5012

DISTRIBUTION STATEMENT:

☒ Approved for public release; distribution unlimited

The views, opinions and/or findings contained in this report are those of the author(s) and should not be construed as an official Department of the Army position, policy or decision unless so designated by other documentation.

REPORT DOCUMENTATION PAGE

Form Approved
OMB No. 0704-0188

Public reporting burden for this collection of information is estimated to average 1 hour per response, including the time for reviewing instructions, searching existing data sources, gathering and maintaining the data needed, and completing and reviewing this collection of information. Send comments regarding this burden estimate or any other aspect of this collection of information, including suggestions for reducing this burden to Department of Defense, Washington Headquarters Services, Directorate for Information Operations and Reports (0704-0188), 1215 Jefferson Davis Highway, Suite 1204, Arlington, VA 22202-4302. Respondents should be aware that notwithstanding any other provision of law, no person shall be subject to any penalty for failing to comply with a collection of information if it does not display a currently valid OMB control number. **PLEASE DO NOT RETURN YOUR FORM TO THE ABOVE ADDRESS.**

1. REPORT DATE *(DD-MM-YYYY)*
01-10-2009

2. REPORT TYPE
Annual Summary

3. DATES COVERED *(From - To)*
1 Oct 2008- 30 Sep 2009

4. TITLE AND SUBTITLE
Generation of soluble Receptor Activator of NF-kappa B Ligand is critical for osteolytic Bone Metastasis

5a. CONTRACT NUMBER

5b. GRANT NUMBER
W81XWH-08-1-0783

5c. PROGRAM ELEMENT NUMBER

5d. PROJECT NUMBER

5e. TASK NUMBER

5f. WORK UNIT NUMBER

6. AUTHOR(S)

Email: KNANNURU@UNMC.EDU

KALYAN C. NANNURU

7. PERFORMING ORGANIZATION NAME(S) AND ADDRESS(ES)

University of Nebraksa Medical Center

Omaha, NE 68198-5900

8. PERFORMING ORGANIZATION REPORT NUMBER

9. SPONSORING / MONITORING AGENCY NAME(S) AND ADDRESS(ES)

U.S. Army Medical Research and Materiel Command
Fort Detrick, Maryland 21702-5012

10. SPONSOR/MONITOR'S ACRONYM(S)

11. SPONSOR/MONITOR'S REPORT NUMBER(S)

12. DISTRIBUTION / AVAILABILITY STATEMENT

Approved for public release; distribution unlimited

13. SUPPLEMENTARY NOTES

14. ABSTRACT

Metastasis is an ominous sign in the progression breast cancer and bone is the most common site of metastasis in advanced disease. The bone microenvironment plays a critical role in tumor-induced osteolysis and osteolytic metastasis through tumor–bone (TB)-interaction. Receptor activator of nuclear factor-κB (RANK) ligand (RANKL) is one of the critical signaling molecules involved in osteolysis and bone metastasis. However, the regulation and functional significance of RANKL at the TB-interface in tumor induced osteolysis remains unclear. In this report, we examined the role of tumor–stromal interaction in the regulation of RANKL expression and its functional significance in tumor-induced osteolysis. Using a novel mammary tumor model, we identified that RANKL expression was upregulated at the TB-interface as compared to the tumor alone area. We demonstrate increased generation of sRANKL at the TB-interface, which is associated with tumor-induced osteolysis. Moreover, we showed that cathepsin G is capable of shedding the extracellular domain of RANKL, generating active sRANKL that is capable of inducing differentiation and activation of osteoclast precursors. Targeting RANKL expression with antisense oligonucleotides (RANKL-ASO) decreased RANKL expression and reduced osteoclast activation at TB interface leading to a significant inhibition in tumor-induced osteolysis.

15. SUBJECT TERMS
Tumor-stromal interaction, RANKL sRANKL osteolysis breast cancer

16. SECURITY CLASSIFICATION OF:			17. LIMITATION OF ABSTRACT	18. NUMBER OF PAGES	19a. NAME OF RESPONSIBLE PERSON
					USAMRMC
a. REPORT	b. ABSTRACT	c. THIS PAGE	UU	38	19b. TELEPHONE NUMBER *(include area code)*
U	U	U			

Standard Form 298 (Rev. 8-98)
Prescribed by ANSI Std. Z39.18

Table of Contents

	Page
Introduction…….……..…..	**4**
Body……..	**5**
(Results/Discussion)	
Key Research Accomplishments…….……..	**12**
Reportable Outcomes……	**12**
Conclusion……	**12**
References…….	**13**
Appendices Index……	**15**
Appendix A……...	**16**
Appendix B……...	**28**
Appendix C……...	**37**

Introduction:

Breast cancer is the most common cancer among women in the United States. Annually, breast cancer is responsible for over 40,000 deaths, making it the second leading cause of cancer death (Jemal *et al.*, 2008). Majority of the complications in breast cancer patients are mainly due to its spread to the distant organs rather than the primary tumor itself. Breast cancer cells are known to metastasize to different organs including lymphnode, lung, liver and bone. Breast cancer cells demonstrate strong predilection for metastasis to bone resulting in lesions that are predominantly osteolytic. Osteolytic bone metastasis causes severe consequences in patients including intractable bone pain, anemia, hypercalcemia, increasing the risk of pathologic fracture and dramatically increase the risk of mortality. Overall these lesions significantly reduce the quality of life of the patient (Mundy, 2002;Boyce *et al.*, 1999;Coleman, 1997).

Arrival of malignant breast cancer cells in to bone microenvironment initiates a vicious cycle of bidirectional communication between tumor and stromal cells that promotes osteolytic metastases (Mundy, 2002;Kakonen and Mundy, 2003;Roodman, 2004). One of the critical signaling molecules involved in this cycle is receptor activator of NF-κB ligand (RANKL). RANKL is a membrane-bound protein expressed on the cell surface of osteoblasts and bone marrow stromal cells (Roodman, 2004;Lacey *et al.*, 2000;Dougall and Chaisson, 2006;Morrissey *et al.*, 2007). Binding of RANKL to its receptor, RANK, expressed on the surface of osteoclast precursors leads to their differentiation into mature osteoclasts (Lacey *et al.*, 2000;Dougall and Chaisson, 2006;Dallas *et al.*, 2002). Another molecule intimately tied to the RANKL-RANK signaling axis is osteoprotegerin (OPG) which is a soluble, decoy receptor of RANKL that prevents RANKL from engaging RANK and initiating signaling (Lacey *et al.*, 2000;Dougall and Chaisson, 2006;Lacey *et al.*, 1998). Malignant cells secrete soluble factors such as parathyroid hormone related peptide (PTHrP) that up-regulates RANKL expression (Kitazawa and Kitazawa, 2002) and enhanced RANKL signaling appears to be the driving force behind tumor-induced osteolytic lesions (Kitazawa and Kitazawa, 2002;Tanaka *et al.*, 2005;Roodman and Dougall, 2008;Zhang *et al.*, 2001;Zhang *et al.*, 2003;Morony *et al.*, 2001). However, very little is known about the role of tumor-bone interaction in regulation of RANKL expression.

While RANKL-RANK signaling is critical to the osteolytic metastasis, it is also the rate limiting step of the cycle since signaling requires cell to cell contact to bring both membrane-bound proteins into contact. One mechanism by which this requirement can be bypassed is the generation of a soluble form of RANKL (sRANKL) that allows widespread osteoclast activation. Other proteases known to be capable of generating sRANKL include matrix metalloproteinase (MMP)3, MMP7, a disintegrin and metalloproteinase (ADAM)-17, and ADAM-19 (Lynch *et al.*, 2005;Chesneau *et al.*, 2003;Schlondorff *et al.*, 2001). Inhibition of Cathepsin G significantly reduced mammary tumor-induced osteolysis suggesting the importance of sRANKL (Wilson *et al.*, 2008). However, while the centrality of RANKL-RANK signaling has been clearly established the relative contributions of RANKL and sRANKL during TB-interactions remain unclear.

In our specific aim 1, we sought to determine the functional significance of RANKL during tumor-stromal interaction in mammary tumor-induced osteolytic lesions and the mechanisms of soluble RANKL generation at TB interface. Our data demonstrate upregulation of RANKL expression and generation of sRANKL at the TB-interface in tumor-induced osteolysis. Furthermore, targeting RANKL expression using antisense-RANKL oligonucleotide decreased RANKL levels and RANKL:OPG ratio at the TB-interface and significantly reduced tumor-induced osteolysis.

Results/Discussion:

This past year I have made significant progress towards better understanding of functional significance of RANKL expression and mechanisms of soluble RANKL generation in tumor-bone microenvironment during osteolytic bone metastasis. Unraveling molecular details behind the mechanisms of soluble RANKL generation and its signaling during mammary tumor induced osteolyis will aid in understanding the pathophysiology of bone metastasis in breast cancer.

RANKL is upregulated at the Tumor-bone interface: We utilized microarray analysis to examine the gene expression pattern at the TB-interface compared to the tumor alone area in tumors derived from all three cell lines. We observed a set of 414 genes commonly upregulated among the three cell lines and 27 genes commonly down-regulated among the three cell lines at the TB interface compared to the tumor alone area. RANKL is found to be one of the highly upregulated genes at TB interface (Fig. 1B). We did not observe any significant difference in RANK expression at the TB-interface compared to the tumor alone area. We validated the microarray data using qRTPCR. We observed upregulation of RANKL mRNA at the TB-interface compared to the tumor alone area in all three groups (Fig. 1C).

We further validated upregulation of RANKL at the tumor-bone interface by using immunohistochemical analysis to demonstrate upregulation of RANKL at the protein level. In agreement with the mRNA expression data, we observed higher expression of RANKL protein at the TB-interface (Fig. 1D). Osteoblasts, stromal cells and tumor cells at the TB-interface stained strongly positive for RANKL [Fig. 1D-ii (lower magnification); 1D-iii (higher magnification)]. In contrast, low expression of RANKL was observed in the tumor alone area (Fig. 1D-i).

RANKL, sRANKL and OPG expression at the TB-interface: To attempt to decipher the relative contributions of membrane- bound RANKL and sRANKL at the tumor-bone interface, we next analyzed expression of sRANKL, the cleaved form of membrane-bound RANKL in mice bearing Cl66 tumors. In addition, we also analyzed the expression of OPG, a soluble decoy receptor of RANKL. Expression of both proteins was analyzed using ELISA specific for OPG and RANKL. Similar to RANKL mRNA expression, the levels of RANKL at the TB-interface were significantly higher compared

to the tumor alone area in all tumors examined (Fig. 2A). We did not observe any significant difference in the level of OPG at the TB-interface compared to the tumor alone area.

We then examined the ratio of RANKL to OPG at the TB-interface and tumor alone area. Results shown in Fig. 2B demonstrate an increased RANKL:OPG ratio at the TB-interface compared to the tumor alone area for all tumors. Together, these data demonstrate upregulation of RANKL and likely upregulation of free, active sRANKL during tumor-induced osteolysis.

We further examined the proportions of RANKL and sRANKL at the TB-interface using Western blot analysis with an antibody capable of detecting both full-length, membrane-bound RANKL (*36 kDa) and sRANKL (*24kDa) (Fig. 3A). Similar to ELISA results, a significant difference in the levels of RANKL and sRANKL were observed at the TB-interface compared with the tumor alone area (Fig. 3B). These data further confirmed that in addition to upregulation of RANKL expression, there was also increased generation of sRANKL at the TB-interface of mammary tumor-induced osteolytic lesions.

Generation of RANKL protein: Invitro transcription and translation system was used to generate recombinant RANKL protein. Full-length RANKL cDNA (NM_003701) with an NH_2-terminal His-tag sequence cloned in pReceiver-B01 (GeneCopoeia) plasmid was used to generate RANKL protein using a TnT Quick Coupled Transcription/Translation system (Promega) per manufacturer's protocol using translation grade [^{35}S]methionine (1,175 Ci/mmol at 10 mCi/mL). Two microliters of the reaction mixture were separated on a 12% SDS-polyacrylamide gel and subsequently visualized and photographed with a Typhoon 9410 Variable Mode Imager (GE Healthcare). The resulting translation product was purified with a His-Trap Crude 1-mL column (GE Healthcare) per manufacturer's protocol. The purified protein was then concentrated by using a Centriprep YM-10 spin column (Omicon) and quantified with the BCA Protein Assay kit per manufacturer's protocol (Pierce).

Soluble RANKL generation by proteolytic cleavage of RANKL by Cathepsin G: In our previous work in prostate cancer model we reported that MMP7 plays a role in prostate tumor–induced osteolysis through the cleavage of cell-surface RANKL into a soluble form of RANKL that is capable of enhancing osteoclast differentiation and subsequent osteolysis (Lynch *et al.*, 2005). To determine if any of the proteases that we observed to be up-regulated at the tumor-bone interface play a similar role in mammary tumor–induced osteolysis, the activity of each protease against full-length RANKL was assessed.

Full-length RANKL protein was generated by using an *in vitro* transcription/translation kit. The product was visualized and the expected ~34-kDa protein was seen (Fig. 4A). Although activity against the native substrate of each protease was observed, only cathepsin G generated a soluble version of RANKL (~24 kDa; Fig. 4B). To confirm cathepsin G–mediated cleavage of RANKL, we used TPCK, a cathepsin G inhibitor, before incubation with full-length RANKL protein. TPCK is an inhibitor of the

chymotrypsin-like group of proteases and is a potent inhibitor of cathepsin G (Overall and Blobel, 2007;Selak *et al.*, 1988). We first confirmed the ability of TPCK to inhibit cathepsin G activity against its native substrate, and TPCK effectively inhibited cathepsin G activity. Cathepsin G preincubated with TPCK did not cleave RANKL (Fig. 4C-*ii*). Finally, Western blot analysis with an anti-RANKL antibody that recognizes an epitope near the COOH terminus confirmed that the cleaved protein was RANKL and that the soluble product generated was derived from full-length RANKL cleaved near the NH_2 terminus within the extracellular domain (Fig. 4C-*i*).

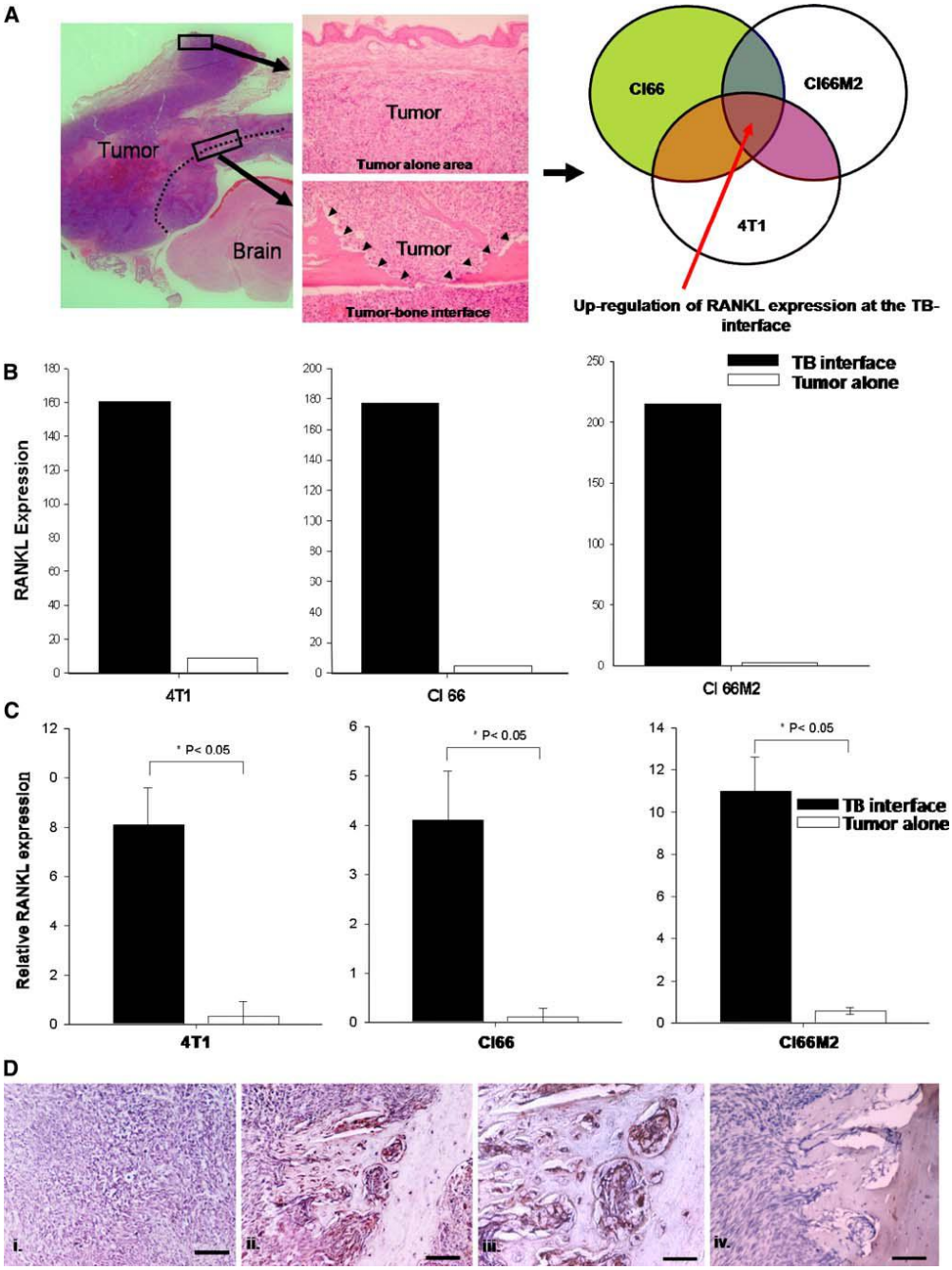

Fig. 1 Upregulation of RANKL expression at the tumor-bone interface. A Samples were microdissected to separate the tumor alone area from the tumor-bone interface for each of the three mammary tumor cell lines. Analysis of Affymetrix Gene Arrays from these samples identified upregulated genes. RANKL was among the genes commonly upregulated at the tumor-bone interface in all three cell lines. B Microarray analysis demonstrated that RANKL is upregulated at the tumor-bone interface in all three cell lines. C qRTPCR confirmed that RANKL is upregulated at the tumor-bone interface in all three cell lines. The values are mean SEM. This is a representative of three experiments with similar results. D Immunohistochemistry of tumor sections stained with RANKL specific antibody depicts increased RANKL staining at the tumor-bone interface (ii 200X; iii 400X) compared to the tumor alone area (i 200X), antibody control shows no non specific staining (iv 200X). Scale bars represent 0.01 mm

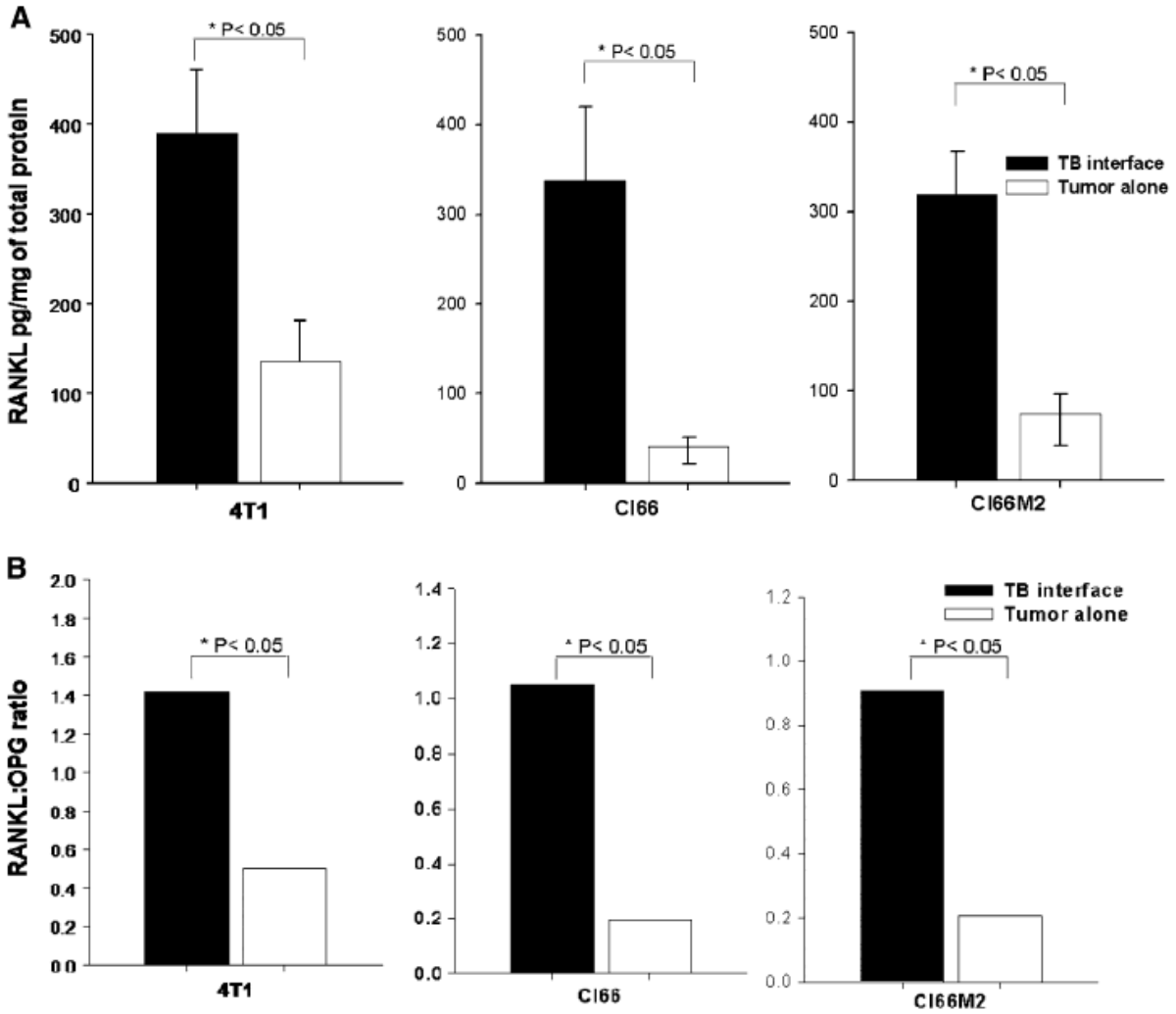

Fig. 2 RANKL and OPG levels at the tumor-bone interface. RANKL was upregulated at the tumor-bone interface compared to the tumor alone area (**A**) as demonstrated by ELISA. **B** . The RANKL:OPG ratio was significantly increased at the tumor-bone interface compared to the tumor alone area in all three cell lines used. The values are mean SEM. This is a representative of three experiments with similar results

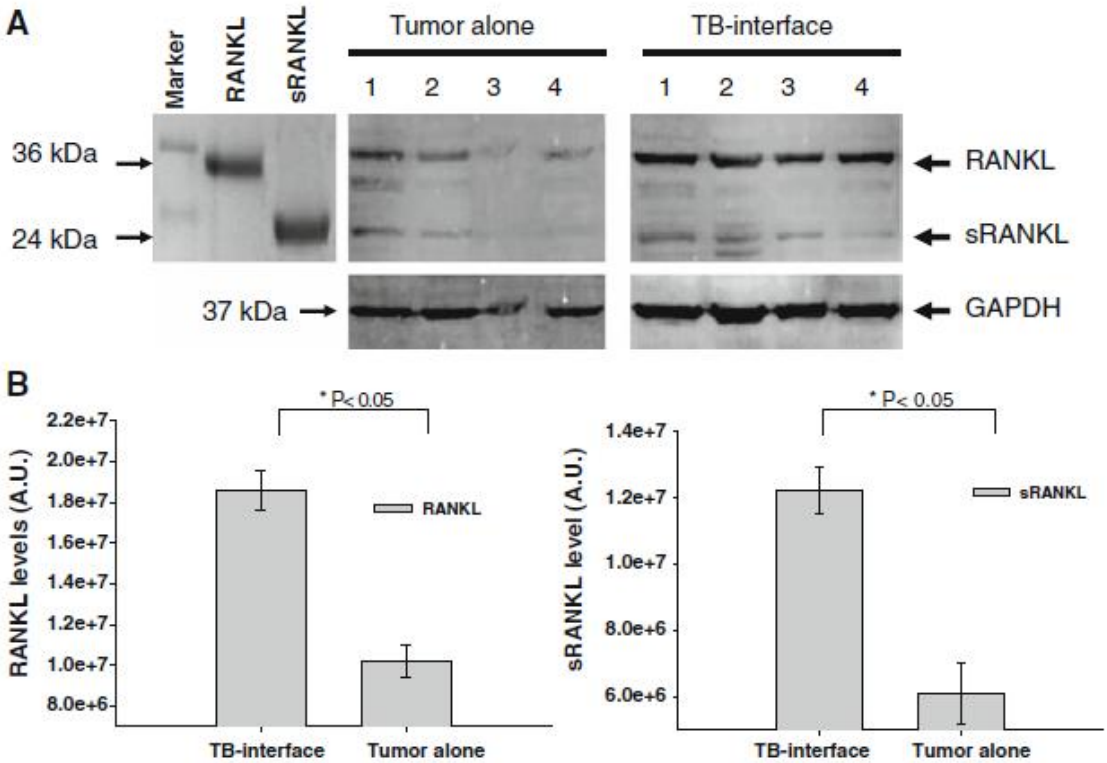

Fig. 3 RANKL and sRANKL proteins during tumor-induced osteolysis. A Tissue lysates from tumor alone areas and TBinterface from four different mice (indicated as 1,2,3 and 4) bearing Cl66 tumors were examined for RANKL and sRANKL levels using Western blot analysis. The antibody used in the analysis detects *36 kDa (membrane bound RANKL) and *24 kDa (sRANKL). B Quantitation of the levels of RANKL and sRANKL was performed using ImageQuant analysis software (GE Biosciences). The levels of RANKL and sRANKL were determined as presented as arbitrary units (A.U.). The values are mean SEM. This is a representative of three experiments with similar results

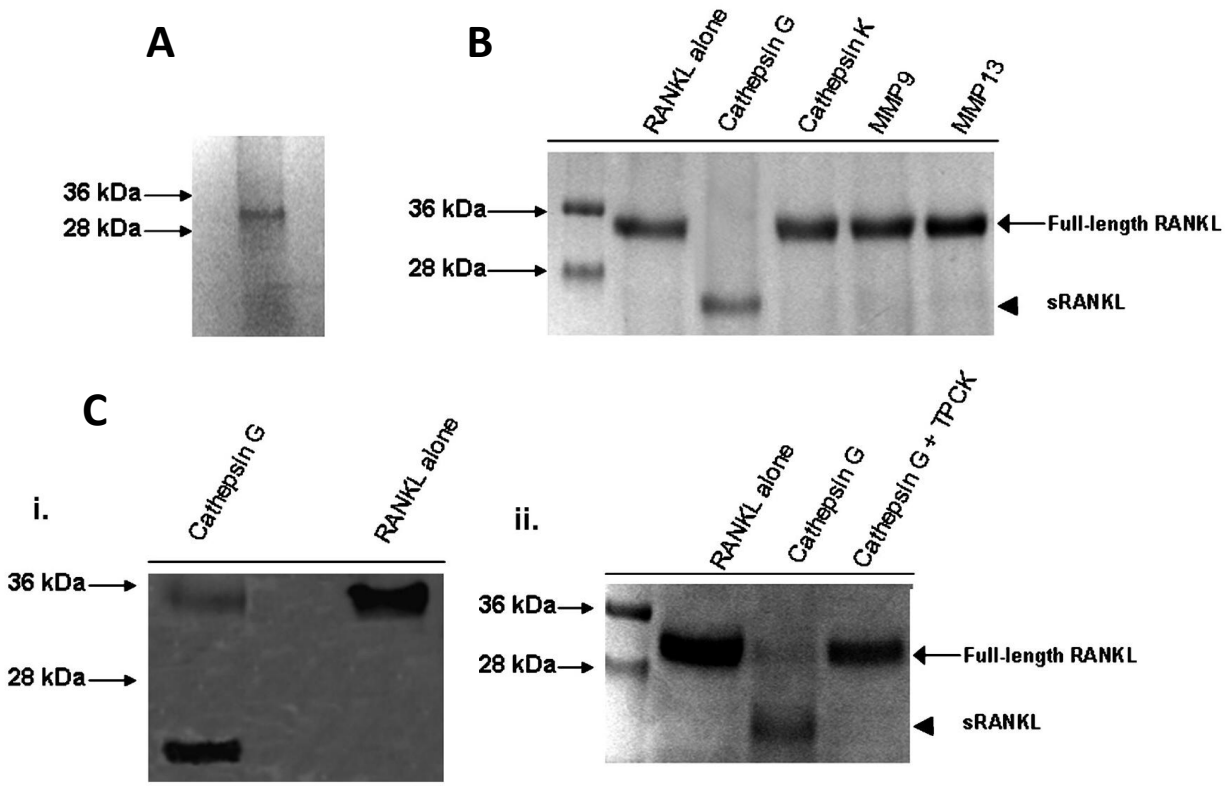

Figure 4. Cathepsin G–dependent generation of sRANKL. *A*, RANKL was generated by using an *in vitro* transcription/translation kit and then purified. A single band at 34 kDa is appropriate for RANKL and shows the purity of the sample. *C*, cathepsin G incubated with full-length RANKL (*arrow*) generated a soluble 24-kDa product (*arrowhead*). *C*, *i*, Western blot with anti-RANKL antibody directed at an epitope at the COOH terminus confirms that cathepsin G cleaves RANKL near the NH_2 terminus. *ii*, TPCK, a cathepsin G inhibitor, blocked cleavage of RANKL, confirming that cathepsin G is responsible for the generation of sRANKL.

Key Research Accomplishments:

- In our study to elucidate the molecular signaling mechanisms that regulate osteolytic bone metastasis in breast cancer,
- We could able to provide importance of soluble RANKL and the mechanism for its generation at tumor-bone interface.
- We have observed upregulation of RANKL at tumor-bone interface compared to tumor alone area both at mRNA level and protein levels.
- Soluble RANKL generation is higher in tumor-bone lysates compared tumor alone samples.
- Soluble RANKL is generated from proteolytic cleavage of full length RANKL near the NH_2 terminus within the extracellular domain by Cathepsin G.
- Increased expression and shedding of RANKL at tumor-bone interface is associated with increased osteoclast activation leading to tumor induced osteolysis.
- We have also shown that targeting RANKL expression in osteolytic bone metastasis model significantly decreases RANKL levels at TB interface and inhibits activation of osteoclasts leading to abrogation of tumor induced osteolysis.

Reportable Outcomes:
Findings from this research work were published in two manuscripts in peer reviewed journals.

Publications:

1. **Nannuru KC**, Futakuchi M, Sadanandam A, Wilson TJ, Varney ML, Myers KJ, et al. Enhanced expression and shedding of receptor activator of NF-kappaB ligand during tumor-bone interaction potentiates mammary tumor-induced osteolysis. *Clin Exp Metastasis 2009 DOI: 10.1007/s10585-009-9279-2, 2009.*

2. Wilson TJ, **Nannuru KC**, Futakuchi M, Sadanandam A, Singh RK. Cathepsin G enhances mammary tumor-induced osteolysis by generating soluble receptor activator of nuclear factor-kappaB ligand. *Cancer Res 2008;68:5803-11*.

Conclusions:

In our study, we sought to determine the functional significance of RANKL during tumor-stromal interaction in mammary tumor-induced osteolytic lesions. Our data demonstrate upregulation of RANKL expression and generation of sRANKL at the TB-interface in tumor-induced osteolysis. Moreover, we showed that cathepsin G is capable of shedding the extracellular domain of RANKL, generating active sRANKL that is capable of inducing differentiation and activation of osteoclast precursors. Targeting RANKL expression using antisense-RANKL oligonucleotide decreased RANKL levels and RANKL:OPG ratio at the TB- interface and significantly reduced tumor-induced osteolysis.

Reference List:

Boyce BF, Yoneda T, Guise TA (1999) Factors regulating the growth of metastatic cancer in bone. *Endocr Relat Cancer* **6** (3): 333-347

Chesneau V, Becherer JD, Zheng Y, Erdjument-Bromage H, Tempst P, Blobel CP (2003) Catalytic Properties of ADAM19. *J Biol Chem* **278** (25): 22331-22340

Coleman RE (1997) Skeletal complications of malignancy. *Cancer* **80** (8 Suppl): 1588-1594

Dallas SL, Rosser JL, Mundy GR, Bonewald LF (2002) Proteolysis of latent transforming growth factor-beta (TGF-beta)-binding protein-1 by osteoclasts. A cellular mechanism for release of TGF-beta from bone matrix. *J Biol Chem* **277** (24): 21352-21360

Dougall WC, Chaisson M (2006) The RANK/RANKL/OPG triad in cancer-induced bone diseases. *Cancer Metastasis Rev* **25** (4): 541-549

Jemal A, Siegel R, Ward E, Hao Y, Xu J, Murray T, Thun MJ (2008) Cancer Statistics, 2008. *CA Cancer J Clin* **58** (2): 71-96

Kakonen SM, Mundy GR (2003) Mechanisms of osteolytic bone metastases in breast carcinoma. *Cancer* **97** (3 Suppl): 834-839

Kitazawa S, Kitazawa R (2002) RANK ligand is a prerequisite for cancer-associated osteolytic lesions. *J Pathol* **198** (2): 228-236

Lacey DL, Tan HL, Lu J, Kaufman S, Van G, Qiu W, Rattan A, Scully S, Fletcher F, Juan T, Kelley M, Burgess TL, Boyle WJ, Polverino AJ (2000) Osteoprotegerin ligand modulates murine osteoclast survival in vitro and in vivo. *Am J Pathol* **157** (2): 435-448

Lacey DL, Timms E, Tan H-L, Kelley MJ, Dunstan CR, Burgess T, Elliott R, Colombero A, Elliott G, Scully S, Hsu H, Sullivan J, Hawkins N, Davy E, Capparelli C, Eli A, Qian Y-X, Kaufman S, Sarosi I, Shalhoub V, Senaldi G, Guo J, Delaney J, Boyle WJ (1998) Osteoprotegerin Ligand Is a Cytokine that Regulates Osteoclast Differentiation and Activation. *Cell* **93** (2): 165-176

Lynch CC, Hikosaka A, Acuff HB, Martin MD, Kawai N, Singh RK, Vargo-Gogola TC, Begtrup JL, Peterson TE, Fingleton B, Shirai T, Matrisian LM, Futakuchi M (2005) MMP-7 promotes prostate cancer-induced osteolysis via the solubilization of RANKL. *Cancer Cell* **7** (5): 485-496

Morony S, Capparelli C, Sarosi I, Lacey DL, Dunstan CR, Kostenuik PJ (2001) Osteoprotegerin inhibits osteolysis and decreases skeletal tumor burden in syngeneic and nude mouse models of experimental bone metastasis. *Cancer Res* **61** (11): 4432-4436

Morrissey C, Kostenuik P, Brown L, Vessella R, Corey E (2007) Host-derived RANKL is responsible for osteolysis in a C4-2 human prostate cancer xenograft model of experimental bone metastases. *BMC Cancer* **7** (1): 148, doi:10.1186/1471-2407-7-148

Mundy GR (2002) Metastasis to bone: causes, consequences and therapeutic opportunities. *Nat Rev Cancer* **2** (8): 584-593

Overall CM, Blobel CP (2007) In search of partners: linking extracellular proteases to substrates. *Nat Rev Mol Cell Biol* **8** (3): 245-257

Roodman GD (2004) Mechanisms of bone metastasis. *N Engl J Med* **350** (16): 1655-1664

Roodman GD, Dougall WC (2008) RANK ligand as a therapeutic target for bone metastases and multiple myeloma. *Cancer Treatment Reviews* **34** (1): 92-101

Schlondorff J, Lum L, Blobel CP (2001) Biochemical and Pharmacological Criteria Define Two Shedding Activities for TRANCE/OPGL That Are Distinct from the Tumor Necrosis Factor alpha Convertase. *J Biol Chem* **276** (18): 14665-14674

Selak MA, Chignard M, Smith JB (1988) Cathepsin G is a strong platelet agonist released by neutrophils. *Biochem J* **251** (1): 293-299

Tanaka S, Nakamura K, Takahasi N, Suda T (2005) Role of RANKL in physiological and pathological bone resorption and therapeutics targeting the RANKL-RANK signaling system. *Immunol Rev* **208:30-49.** 30-49

Wilson TJ, Nannuru KC, Futakuchi M, Sadanandam A, Singh RK (2008) Cathepsin G Enhances Mammary Tumor-Induced Osteolysis by Generating Soluble Receptor Activator of Nuclear Factor-{kappa}B Ligand. *Cancer Res* **68** (14): 5803-5811

Zhang J, Dai J, Qi Y, Lin DL, Smith P, Strayhorn C, Mizokami A, Fu Z, Westman J, Keller ET (2001) Osteoprotegerin inhibits prostate cancer-induced osteoclastogenesis and prevents prostate tumor growth in the bone. *J Clin Invest* **107** (10): 1235-1244

Zhang J, Dai J, Yao Z, Lu Y, Dougall W, Keller ET (2003) Soluble receptor activator of nuclear factor kappaB Fc diminishes prostate cancer progression in bone. *Cancer Res* **63** (22): 7883-7890

Appendices:

A. **Nannuru KC**, Futakuchi M, Sadanandam A, Wilson TJ, Varney ML, Myers KJ, et al. Enhanced expression and shedding of receptor activator of NF-kappaB ligand during tumor-bone interaction potentiates mammary tumor-induced osteolysis. *Clin Exp Metastasis 2009 DOI: 10.1007/s10585-009-9279-2, 2009.*

B. Wilson TJ, **Nannuru KC**, Futakuchi M, Sadanandam A, Singh RK. Cathepsin G enhances mammary tumor-induced osteolysis by generating soluble receptor activator of nuclear factor-kappaB ligand. *Cancer Res 2008;68:5803-11*.

C. Current CV

Clin Exp Metastasis
DOI 10.1007/s10585-009-9279-2

RESEARCH PAPER

Enhanced expression and shedding of receptor activator of NF-κB ligand during tumor–bone interaction potentiates mammary tumor-induced osteolysis

Kalyan C. Nannuru · Mitsuru Futakuchi · Anguraj Sadanandam · Thomas J. Wilson · Michelle L. Varney · Kathleen J. Myers · Xiaodong Li · Eric G. Marcusson · Rakesh K. Singh

Received: 28 April 2009 / Accepted: 23 June 2009
© Springer Science+Business Media B.V. 2009

Abstract The bone microenvironment plays a critical role in tumor-induced osteolysis and osteolytic metastasis through tumor–bone (TB)-interaction. Receptor activator of nuclear factor-κB (RANK) ligand (RANKL) is one of the critical signaling molecules involved in osteolysis and bone metastasis. However, the regulation and functional significance of RANKL at the TB-interface in tumor-induced osteolysis remains unclear. In this report, we examined the role of tumor–stromal interaction in the regulation of RANKL expression and its functional significance in tumor-induced osteolysis. Using a novel mammary tumor model, we identified that RANKL expression was upregulated at the TB-interface as compared to the tumor alone area. We demonstrate increased generation of sRANKL at the TB-interface, which is associated with tumor-induced osteolysis. The ratio of RANKL to osteoprotegrin (OPG), a decoy receptor for RANKL, at the TB-interface was also increased. Targeting RANKL expression with antisense oligonucleotides (RANKL-ASO), significantly abrogated tumor-induced osteolysis, decreased RANKL expression and the RANKL:OPG ratio at the TB-interface. Together, these results demonstrate that upregulation of RANKL expression and sRANKL generation at the TB-interface potentiates tumor-induced osteolysis.

Keywords Bone metastasis · RANKL · Soluble RANKL · Tumor–bone interaction · Tumor-induced osteolysis · Anti-sense therapeutics

K. C. Nannuru · A. Sadanandam · T. J. Wilson · M. L. Varney · R. K. Singh (✉)
Department of Pathology and Microbiology, 985845 Nebraska Medical Center, University of Nebraska Medical Center, Omaha, NE 68198-5845, USA
e-mail: rsingh@unmc.edu

M. Futakuchi
Department of Molecular Toxicology, Nagoya City University, Nagoya City, Nagoya, Japan

K. J. Myers · X. Li · E. G. Marcusson
Isis Pharmaceuticals, Carlsbad, CA, USA

Introduction

Breast cancer is the most common cancer among women in the United States. Annually, breast cancer is responsible for over 40,000 deaths, making it the second leading cause of cancer death [1]. A large portion of breast cancer-related mortality is due to metastatic disease rather than the primary tumor itself. Breast cancer cells demonstrate strong predilection for metastasis to bone resulting in lesions that are predominantly osteolytic. These lesions significantly reduce the quality of life of the patient by causing intractable bone pain, anemia, hypercalcemia, increasing the risk of pathologic fracture and dramatically increase the risk of mortality [2–4].

Malignant breast cancer cells entry to bone microenvironment initiates a vicious cycle of bidirectional communication between tumor and stromal cells that promotes osteolytic metastases [2, 5, 6]. One of the critical signaling molecules involved in this cycle is receptor activator of NF-κB ligand (RANKL). RANKL is a membrane-bound protein expressed on the cell surface of osteoblasts and bone marrow stromal cells [6–9]. Binding of RANKL to its receptor, RANK, expressed on the surface of osteoclast precursors leads to their differentiation into mature

Published online: 10 July 2009

osteoclasts [7, 8, 10]. Another molecule intimately tied to the RANKL-RANK signaling axis is osteoprotegerin (OPG) which is a soluble, decoy receptor of RANKL that prevents RANKL from engaging RANK and initiating signaling [7, 8, 11]. Malignant cells secrete soluble factors such as parathyroid hormone related peptide (PTHrP) that up-regulates RANKL expression [12] and enhanced RANKL signaling appears to be the driving force behind tumor-induced osteolytic lesions [12–17]. However, very little is known about the role of tumor–bone interaction in regulation of RANKL expression.

While RANKL-RANK signaling is critical to the osteolytic metastasis, it is also the rate limiting step of the cycle since signaling requires cell to cell contact to bring both membrane-bound proteins into contact. One mechanism by which this requirement can be bypassed is the generation of a soluble form of RANKL (sRANKL) that allows widespread osteoclast activation. Recently, Cathepsin G was identified as a protein that is upregulated at the TB-interface of mammary tumor-induced osteolytic lesions and was shown to be capable of generating sRANKL [18, 19]. Other proteases known to be capable of generating sRANKL include matrix metalloproteinase (MMP)3, MMP7, a disintegrin and metalloproteinase (ADAM)-17, and ADAM-19 [20–22]. Inhibition of Cathepsin G significantly reduced mammary tumor-induced osteolysis suggesting the importance of sRANKL [18]. However, while the centrality of RANKL-RANK signaling has been clearly established the relative contributions of RANKL and sRANKL during TB-interactions remain unclear.

In the present study, we sought to determine the functional significance of RANKL during tumor–stromal interaction in mammary tumor-induced osteolytic lesions. Our data demonstrate upregulation of RANKL expression and generation of sRANKL at the TB-interface in tumor-induced osteolysis. Furthermore, targeting RANKL expression using antisense-RANKL oligonucleotide decreased RANKL levels and RANKL:OPG ratio at the TB-interface and significantly reduced tumor-induced osteolysis.

Materials and methods

Animal model and tissue sample processing

4T1 (highly metastatic), Cl66 (moderately metastatic), and Cl66M2 (low metastatic), three murine mammary adenocarcinoma cell lines with different metastatic potentials [23–29] syngeneic to BALB/c mice, were used in this study. All cell lines were maintained in Dulbecco's Modified Eagle Media (DMEM) (Mediatech, Hendon, VA) with 5% serum supreme (Biowhitaker, Walkersville, MD), 1% vitamins, 1% L-glutamine, and 0.08% gentamicin (Invitrogen, Carlsbad, CA).

Six to eight week old female BALB/c mice (NCI, Bethesda, MD) were used in this study. All mice were maintained in accordance with the Institutional Animal Use and Care Committee of the University of Nebraska Medical Center. Mammary tumor cells (5×10^4 cells/50μl) mixed in growth-factor reduced Matrigel (BD Biosciences, San Jose, CA) were injected directly onto the calvaria to mimic the close association of tumor cells and cells of the bone microenvironment [12, 18, 20]. Tumor growth was monitored and animals were sacrificed at 4 weeks post-implantation. The tumor and the underlying bone tissues were dissected into two halves, one half being used for histology sections and the other half used for micro-dissecting the tumor alone area and the TB interface for further analysis.

For histological examination and immunohistochemistry, the samples were fixed with periodate-lysine-paraformaldehyde at 4°C for 48 h. The tissues were then transferred into a decalcification solution (15% EDTA with glycerol, pH 7.4) for 4 weeks and were subsequently paraffin embedded and processed for histology.

Total RNA was extracted using Trizol (Invitrogen, Carlsbad, CA) following the manufacturer's instructions. The RNA concentration was quantified using a NANO drop ND-1000 Spectrophotometer (Nano Drop Technologies, Wilmington, DE).

Protein was extracted from the samples using T-PER tissue protein extractor solution (Pierce, Rockford, IL) following the manufacturer's provided protocol. Protein samples were quantified using a BCA protein assay kit (Pierce, Rockford, IL).

Microarray analysis and quantitative real time PCR (qRT-PCR)

Calcified frozen sections were serially sectioned in 10-μm thick slices and at least ten slides per mouse were micro-dissected with careful separation of the TB-interface and the tumor alone areas. Total RNA was extracted from each micro-dissected population, pooled and an equal amount of RNA was amplified using a probe amplification kit (Affymetrix, Santa Clara, CA). An Affymetrix Mouse Expression Array 430 was used for comparing gene expression profiles between the TB-interface and the tumor alone areas. A complete detection and analysis of signals for each chip was performed using Affymetrix GeneChip® Operating Software to generate raw expression data. A signal log ratio algorithm was used to estimate the magnitude of change of a transcript when two arrays are compared (experimental versus baseline). It is calculated by comparing each probe pair on the

experimental array, here the TB-interface, to the corresponding probe pair on the baseline array, here the tumor alone area, and considering the mean of the log ratios of probe pair intensities across the two arrays. The change is expressed as the $\log_2$ ratio. Thus, a signal log ratio of 1.0 indicates an increase of transcript level by twofold and −1.0 indicates a decrease by twofold. For each set of tissue from 4T1, Cl66 and Cl66M2, the signal log ratio of the TB-interface versus the tumor alone area was calculated, and the genes were ordered from highest to lowest expression levels.

Gene expression analysis was confirmed using qRT-PCR for the TB-interface and tumor alone area samples. 5 μg of RNA from each sample was used to synthesize first strand cDNA. 2 μl of 1:100 diluted first strand cDNA were amplified in a 20 μl reaction with SYBR green master mix (Roche, Indianapolis IN) and 10 mM primer mix using a Bio-Rad iCycler (Bio-Rad, Hercules, CA). The following reaction conditions were used: initial denaturation at 95°C for 3 min, followed by amplification cycles with denaturation at 95°C for 60 s, annealing at 60°C for 60 s, and extension at 72°C for 60 s, and finally a long extension at 72°C for 2 min. Primers used for RANKL were 5′-TTA GCA TTC AGG TGT CCA ACC-3′ and 5′-CGT GGG CCA TGT CTC TTA GTA-3′; and for glyceraldehyde-3-phosphate dehydrogenase (GAPDH) were 5′-AGC CTC GTC CCG TAG ACA AAA-3′ and 5′-GAT GAC AAG CTT CCC ATT CTC G-3′. The fluorescence intensity of double-strand specific SYBR Green, reflecting the amount of formed PCR-product, was monitored at the end of each elongation step. The *ct* value for each gene was normalized with GAPDH expression for relative gene expression analysis.

Immunohistochemistry and TRAP staining

RANKL protein expression was evaluated by immunohistochemistry on tumor sections using a RANKL-specific antibody (Santa Cruz Biotechnology, Santa Cruz, CA). The sections were deparaffinized using EZ dewax solution (Biogenex, San Ramon, CA). For antigen retrieval, the sections were boiled in 0.1 M citrate buffer (pH 6.0) for 10 min and endogenous peroxidase activity was blocked using 3% H_2O_2 for 5 min. The sections were then blocked in antibody diluent for 1 h at room temperature. RANKL antibody was diluted 1:100 in blocking solution and sections were incubated overnight at 4°C. After washing, the slides were incubated with anti-goat biotinylated antibody for 30 min at room temperature. After washing, immunoreactivity was detected using Vectastain ABC and DAB substrate kits (Vector Laboratories, Burlingame, CA). Sections were counterstained with hematoxylin, dehydrated, and permanently mounted.

Tartrate resistant acid phosphatase (TRAP) staining was performed to detect activated osteoclasts in vivo according to the manufacturer's instructions (Sigma Chemicals, St. Louis, MO). For quantitative analysis, immunostained sections were examined under a Nikon light microscope. The number of positive cells was assessed at a magnification of 400× for each lesion.

Enzyme linked immunosorbent assay (ELISA) for RANKL and OPG

Quantitative determination of RANKL and OPG levels at the TB-interface and tumor alone area was performed using a commercially available ELISA kit (Biomedica, Vienna, Austria: Cat:BI20522) according to the manufacturer's instructions. Briefly, pre-coated wells were incubated with samples or recombinant standard and biotinylated antibody for 3 h. After washing, the reactivity was detected using streptavidin-HRP conjugate and tetramethylbenzidine substrate solution. The reaction was stopped and absorbance was determined at 450 nm, with correction at 540 nm using an ELx800 ELISA plate reader (BioTek, Winooski, VT). The sensitivity of these kits were 0.4 pmol/l for sRANKL and 0.14 pmol/l for OPG.

Western blot analysis

Tissue lysates (50 μg) from microdissected tumor alone area and TB-interface were separated on a 12% SDS-polyacrylamide gel and then electrotransferred to a PVDF membrane. The membrane was then washed with 0.1% Tween-Tris-buffered saline (TTBS). The membrane was then blocked overnight in 5% bovine serum albumin (BSA) in phosphate buffered saline (PBS) and blotted with 1:500 anti-RANKL antibody that recognizes an epitope near the C-terminus of RANKL (Santa Cruz Biotechnology, Santa Cruz, CA) and anti-GAPDH antibody (Cell Signaling Technology Inc, Danvers, MA) diluted in TTBS. After washing in TTBS, the membrane was incubated for 60 min with 1:1500 anti-goat-HRP diluted in TTBS. Finally, after washing with TTBS, the membrane was developed using an ECL Plus Western Blotting Detection System (GE Healthcare) per manufacturer's protocol and imaged using a Typhoon 9410 Variable Mode Imager (GE Healthcare). The bands for RANKL, sRANKL and GAPDH were quantified and compared using ImageQuant 5.1 (GE Healthcare).

Treatment with antisense oligonucleotides for inhibition of RANKL expression and osteolysis

Antisense oligonucleotides (ASO) used in the therapeutic protocol were obtained from Isis Pharmaceuticals,

Carlsbad, CA. These ASOs, used throughout this study, were designed specific to RANKL. 2′-methoxyethyl modified chimeric ASOs are synthesized as previously described [30]. These oligonucleotides are modified at the 2′ sugar position of the five bases at both the 3′ and 5′ ends with a methoxyethyl group. This modification greatly increases the stability of the oligonucleotides and the affinity for its target mRNA while reducing the amount of immune stimulatory and inflammatory effects that can be seen with oligonucleotides in mice [31]. Active ASOs were identified by screening 46 ASOs designed to be specific for RANKL. These ASOs were transfected into cells and RNA was isolated 24 h later. RANKL mRNA levels were determined by RT-PCR and the most effective ASOs were identified. The efficacy of these ASOs was confirmed in concentration-response experiments and the most potent ASO was used for further experiments. The sequence of this ASO is GTC TTA CAC ATG TAT AGA CA. As a negative control, we used an oligonucleotide with the same chemical modifications, but a sequence, TCT TAT GTT TCC GAA CCG TT, that did not match any known mRNA in the mouse genome.

To determine the effect of inhibition of RANKL expression using ASOs, animals bearing Cl66 mammary tumors were randomly divided into two treatment groups (control-ASO and RANKL-ASO). The oligonucleotides were dissolved in normal saline (0.9% NaCl) and were administered by intraperitoneal (i.p.) injection at a dose of 50 mg/kg/day starting at day 7 following tumor implantation for 5 days with 2 days off followed by another 4 days (see Fig. 5A). Tumor growth was monitored and mice were sacrificed on day 28. Tumor alone and TB-interface samples were collected and processed for further analysis.

Statistical analysis

The significance of the in vitro data was determined by Student's *t*-test (two-tailed) using SPSS software (SPSS, Chicago, IL). In vivo analysis was performed using Wilcoxon signed rank test and Mann–Whitney *U*-test of significance. A value of $P < 0.05$ was deemed significant.

Results

Osteoclast activation and osteolysis is similar between cell lines

Mammary tumor cells 4T1, Cl66, and Cl66M2, were transplanted onto the calvaria of BALB/c mice and tumor growth was monitored. Histochemical analysis demonstrated that all tumors exhibited tumor-induced osteolysis and osteoclast activation similar to that observed in breast cancer bone metastasis (Fig. 1). The degree of osteolysis was assessed by calculating the bone destruction index (BDI), calculated by comparing the ratio of the length of bone completely destroyed by the tumor cells to the total length of the bone at the tumor-bone interface (Fig. 1B). We did not observe any difference in bone destruction index between the three cell lines with the BDI being 45–50% for all three cell lines (Fig. 1B). Similarly, we observed no significant difference in the number of TRAP-positive osteoclasts at the tumor-bone interface among tumors from the three different cell lines (Fig. 1C, D). Furthermore, the number of osteoclasts at the TB-interface was associated with the bone destruction index (Fig. 1B, D).

RANKL is upregulated at the tumor-bone interface

We utilized microarray analysis to examine the gene expression pattern at the TB-interface compared to the tumor alone area in tumors derived from all three cell lines (Fig. 2). We observed a set of 414 genes commonly upregulated among the three cell lines and 27 genes commonly down-regulated among the three cell lines at the TB-interface compared to the tumor alone area. Three highly upregulated genes included integrin binding bone sialoprotein, RANKL, and MMP13. From these genes, we selected RANKL for further analysis (Fig. 2A, B). We did not observe any significant difference in RANK expression at the TB-interface compared to the tumor alone area (data not shown). We validated the microarray data using qRT-PCR. We observed upregulation of RANKL mRNA at the TB-interface compared to the tumor alone area in all three groups (Fig. 2C).

We further validated upregulation of RANKL at the tumor-bone interface by using immunohistochemical analysis to demonstrate upregulation of RANKL at the protein level. In agreement with the mRNA expression data, we observed higher expression of RANKL protein at the TB-interface (Fig. 2D). Osteoblasts, stromal cells and tumor cells at the TB-interface stained strongly positive for RANKL [Fig. 2D-ii (lower magnification); 2D-iii (higher magnification)]. In contrast, low expression of RANKL was observed in the tumor alone area (Fig. 2D-i).

RANKL, sRANKL and OPG expression at the TB-interface

To attempt to decipher the relative contributions of membrane-bound RANKL and sRANKL at the tumor-bone interface, we next analyzed expression of sRANKL, the cleaved form of membrane-bound RANKL in mice bearing Cl66 tumors. In addition, we also analyzed the expression of OPG, a soluble decoy receptor of RANKL. Expression

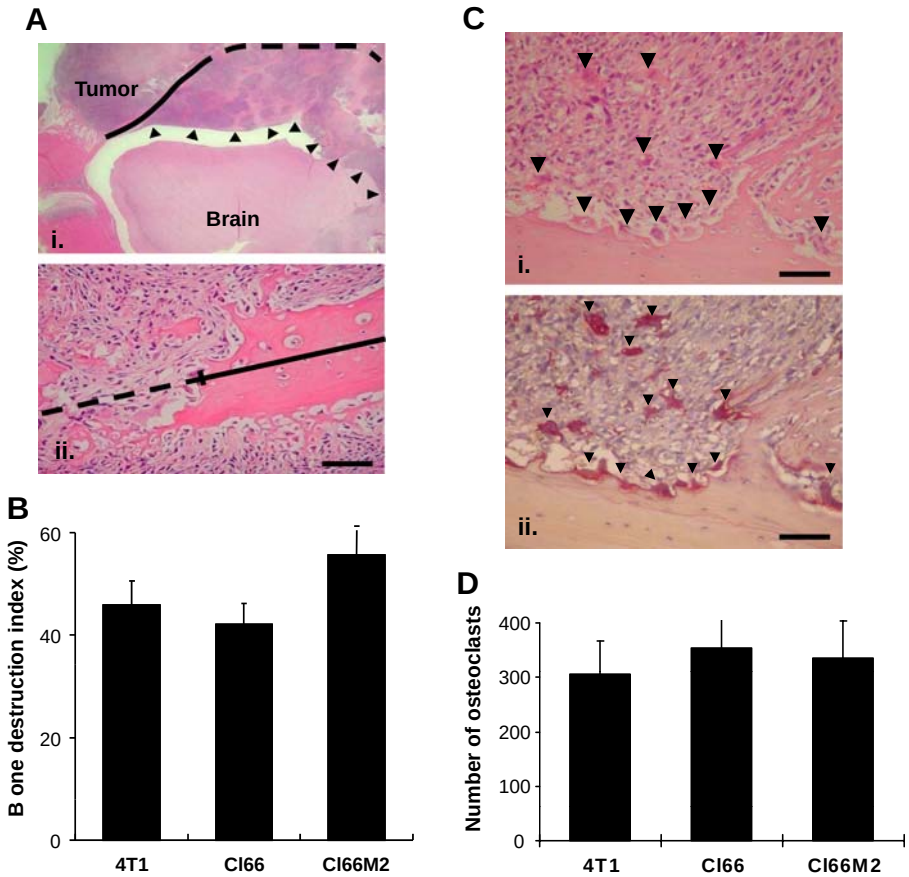

Fig. 1 Mammary tumor-induced osteolytic changes. **A** H&E staining of the tumor bone interface from Cl66 tumors implanted mice; **i** low magnification (20×); **ii** higher magnification (200×) to demonstrate the tumor-bone interface. The levels of tumor-induced osteolysis in H&E-stained sections were measured by comparing length of the completely resorbed bone (*dotted line*) and areas of no bone destruction (*solid lines*). Arrows indicate cranial invasion and growth of tumors. **B** The bone destruction index in 4T1, Cl66 and Cl66M2 tumors. BDI was measured on at least two different sections for each mice and average value of BDI calculated from the measurements of all the mice in the group. **C i** H&E-stained section to demonstrate the presence of osteoclasts at the Tumor Bone interface during intracranial penetration and growth of tumor (*arrows heads*); **ii** TRAP-positive multinucleated cells as osteoclasts counted along the total length of the TB-interface (*arrow heads*). **D** The number of TRAP-positive osteoclasts in 4T1, Cl66 and Cl66M2 tumors. The values are mean ± SEM ($n = 5$ mice per group). *Scale bars* represent 0.01 mm

of both proteins was analyzed using ELISA specific for OPG and RANKL. Similar to RANKL mRNA expression, the levels of RANKL at the TB-interface were significantly higher compared to the tumor alone area in all tumors examined (Fig. 3A). We did not observe any significant difference in the level of OPG at the TB-interface compared to the tumor alone area (data not shown).

We then examined the ratio of RANKL to OPG at the TB-interface and tumor alone area. Results shown in Fig. 3B demonstrate an increased RANKL:OPG ratio at the TB-interface compared to the tumor alone area for all tumors. Together, these data demonstrate upregulation of RANKL and likely upregulation of free, active sRANKL during tumor-induced osteolysis.

We further examined the proportions of RANKL and sRANKL at the TB-interface using Western blot analysis with an antibody capable of detecting both full-length, membrane-bound RANKL (~36 kDa) and sRANKL (~24kDa) (Fig. 4A). Similar to ELISA results, a significant difference in the levels of RANKL and sRANKL were observed at the TB-interface compared with the tumor alone area (Fig. 4B). These data further confirmed that in addition to upregulation of RANKL expression, there was also increased generation of sRANKL at the TB-interface of mammary tumor-induced osteolytic lesions.

Inhibiting RANKL expression abrogates mammary tumor-induced osteolysis

Next, we evaluated the functional significance of enhanced RANKL expression and increased soluble

RANKL levels during tumor–bone interaction. To determine the functional role of RANKL and soluble RANKL in tumor induced osteolysis, we used ASOs to knock down RANKL expression in Cl66 tumor bearing mice. We did not observe any weight loss or toxicity in any of the treatment groups (data not shown). In addition, we did not observe any significant difference in tumor growth between RANKL-ASO and control-ASO groups (data not shown).

H&E staining of tumor sections demonstrated severe bone destruction in control-ASO treated tumors (Fig. 5B-i) whereas RANKL-ASO treated tumors showed very little or no osteolysis (Fig. 5B-ii). We observed a significant inhibition in RANKL expression at the TB-interface in RANKL-ASO treated group as compared to control-ASO treated group (Fig. 5F). We quantified the severity of lesion by measuring bone destruction index and observed a significant decrease in osteolysis in the RANKL-ASO treated group compared to the control-ASO treated group (Fig. 5C). Activated osteoclasts are responsible for osteolysis, hence we analyzed whether RANKL targeting has any effect on osteoclast activation and number at the tumor bone interface. TRAP staining was used to enumerate activated osteoclasts at the TB interface (Fig. 5D). We observed a significant decrease in activated osteoclasts per microscopic field at the TB interface in RANKL-ASO treated mice compared to control-ASO treated group (Fig. 5E). Decreased osteoclast number observed in RANKL-ASO treated group is in association with inhibition of tumor induced osteolysis.

We then examined the expression of RANKL in tumors from RANKL-ASO and control-ASO treated animals using qRT-PCR. The expression of RANKL at the TB-interface was significantly lower in the RANKL-ASO treated group as compared to the control-ASO treated group (Fig. 5F). We observed low levels of RANKL expression in the tumor alone area which was not altered by RANKL-ASO treatment (Fig. 5F).

Next, we analyzed the effect of RANKL-ASO on the levels of RANKL and OPG proteins in tumors. Similar to RANKL mRNA expression, knocking down expression of RANKL using RANKL-ASO inhibited RANKL protein levels at the TB-interface (Fig. 6A). We also observed a concomitant increase (but not significantly different) in the level of OPG at the TB-interface in the RANKL-ASO treated group compared to the control-ASO treatment (Fig. 6B).

With a decrease in RANKL at the TB-interface of RANKL-ASO treated animals, there was a significant decrease in the RANKL:OPG ratio following RANKL-ASO treatment (Fig. 6C). These studies demonstrate that knocking down RANKL expression at the TB-interface inhibits generation of RANKL, decreases RANKL to OPG ratios, and inhibits mammary tumor-induced osteolysis.

Discussion

Breast cancer bone metastasis depends on the interaction of tumor cells with the bone microenvironment which triggers a 'vicious cycle' leading to osteoclast activation and bone destruction [5, 32, 33]. The cellular and molecular regulators of tumor–stromal interaction in osteolytic bone metastasis remain unclear. Understanding the bidirectional communication that occurs between tumor cells and bone stromal cells has the potential to reveal potential therapeutic targets that would abrogate osteolysis and significantly improve the quality of life for breast cancer patients.

Using a syngeneic murine model and three mammary tumor cell lines, we demonstrated that RANKL expression was commonly up-regulated at the TB-interface as compared to the tumor alone area. Several studies have implicated the role of RANKL in the vicious cycle of osteolytic bone metastasis [34]. RANKL is the key stimulator of bone resorption; however, the relative abundance and importance of RANKL produced by malignant cells and host cells during tumor–bone interaction remains unclear. In the present study, we demonstrated that RANKL is predominantly expressed at the TB-interface. Both tumor cells and bone stromal cells, including osteoblasts at the TB-interface, expressed RANKL. This data agrees with a recent report in a prostate cancer model that utilized a xenograft model of human tumor cells into a murine host to decipher the relative contributions of RANKL from the tumor cells versus the bone stromal cells [9]. In contrast, we observed very little RANKL expression in the tumor alone areas. The expression of RANKL at the TB-interface coincided

Fig. 2 Upregulation of RANKL expression at the tumor-bone interface. **A** Samples were microdissected to separate the tumor alone area from the tumor-bone interface for each of the three mammary tumor cell lines. Analysis of Affymetrix Gene Arrays from these samples identified upregulated genes. RANKL was among the genes commonly upregulated at the tumor-bone interface in all three cell lines. **B** Microarray analysis demonstrated that RANKL is upregulated at the tumor-bone interface in all three cell lines. **C** qRT-PCR confirmed that RANKL is upregulated at the tumor-bone interface in all three cell lines. The values are mean ± SEM. This is a representative of three experiments with similar results. **D** Immunohistochemistry of tumor sections stained with RANKL specific antibody depicts increased RANKL staining at the tumor-bone interface (**ii** 200×; **iii** 400×) compared to the tumor alone area (**i** 200×), antibody control shows no non specific staining (**iv** 200×). *Scale bars* represent 0.01 mm

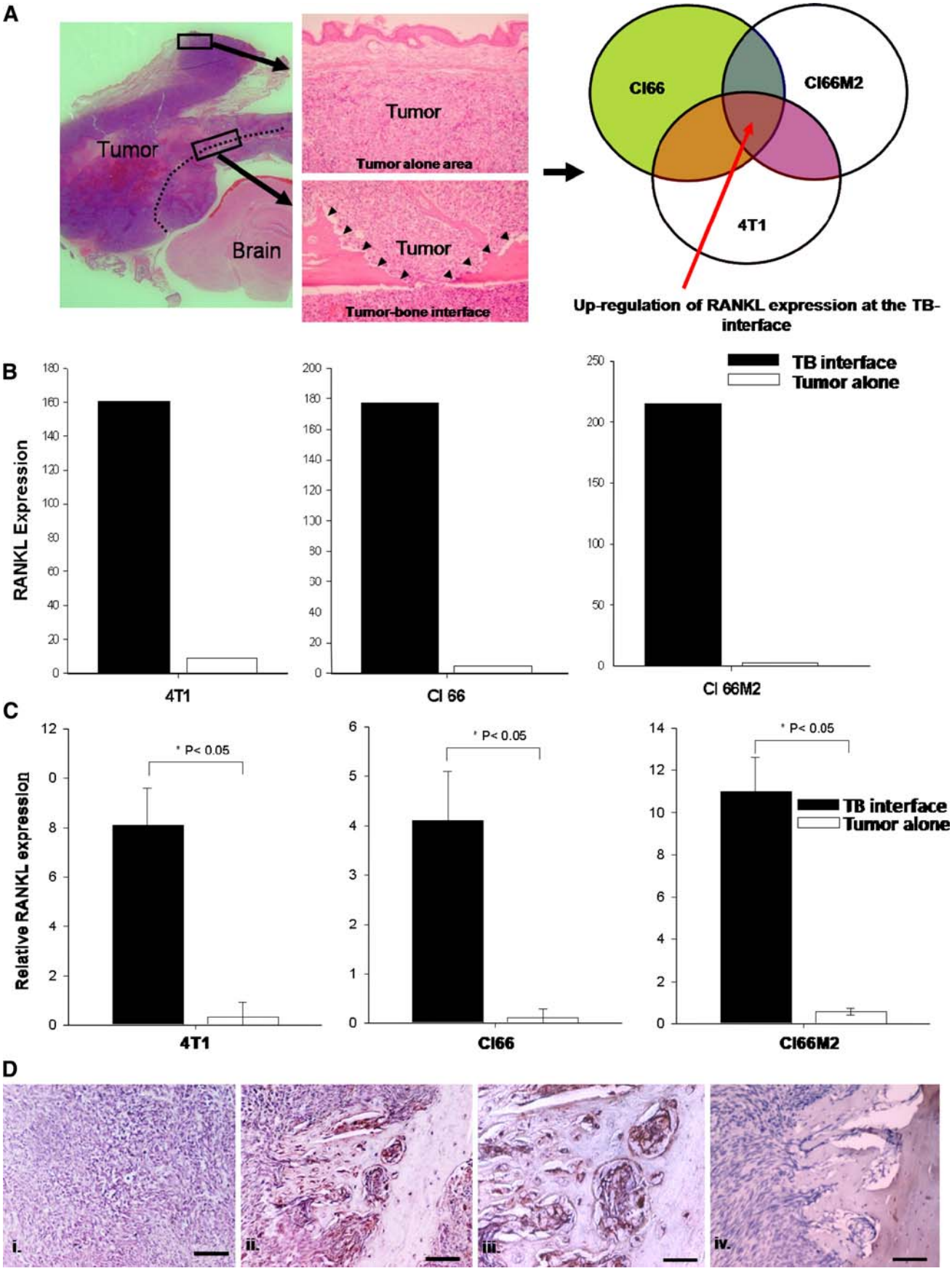
A
Tumor
Brain
Tumor
Tumor alone area
Tumor
Tumor-bone interface
CI66
CI66M2
4T1
Up-regulation of RANKL expression at the TB-interface
B
RANKL Expression
TB interface
Tumor alone
4T1
CI 66
CI 66M2
C
Relative RANKL expression
* P< 0.05
* P< 0.05
* P< 0.05
TB interface
Tumor alone
4T1
CI66
CI66M2
D
i.
ii.
iii.
iv.

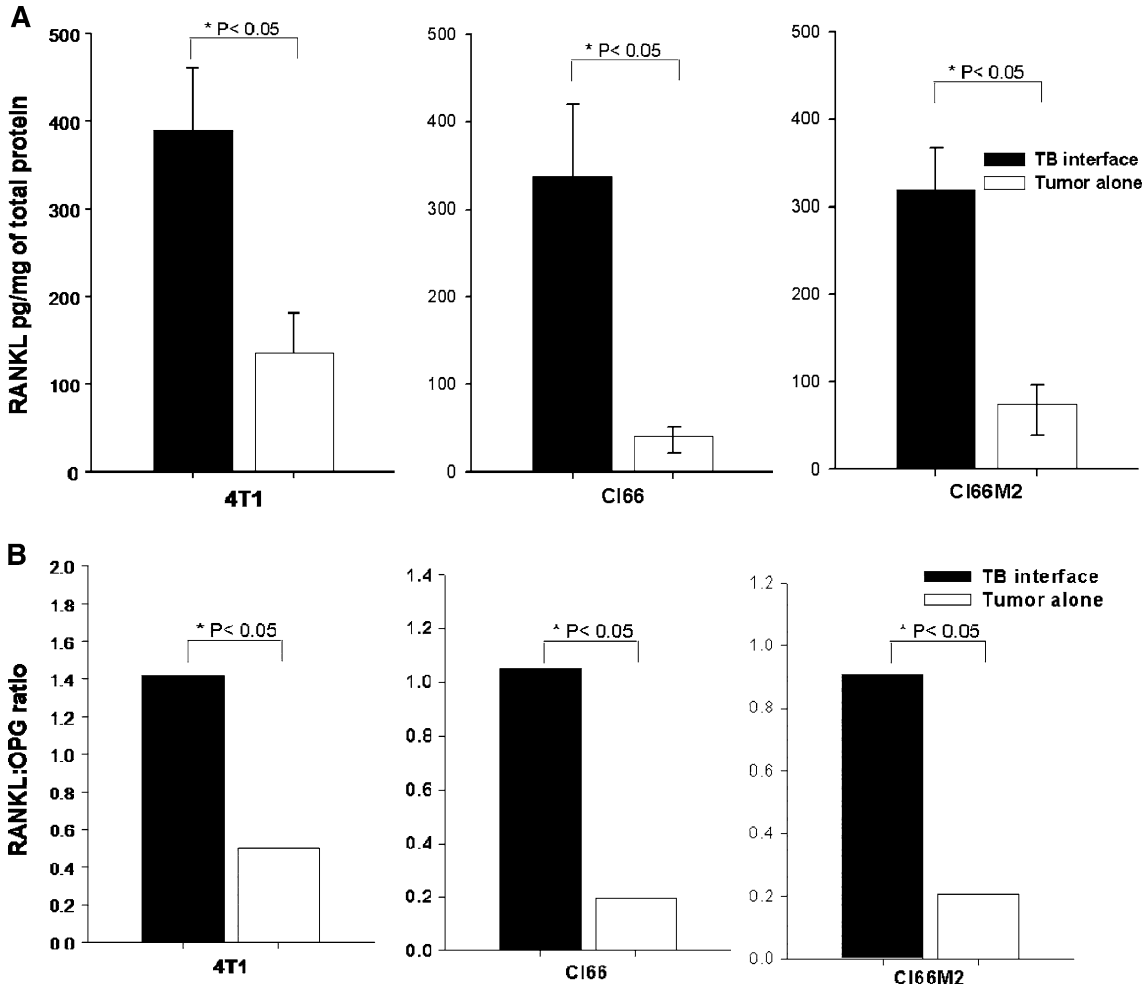

Fig. 3 RANKL and OPG levels at the tumor-bone interface. RANKL was upregulated at the tumor-bone interface compared to the tumor alone area (**A**) as demonstrated by ELISA. **B** The RANKL:OPG ratio was significantly increased at the tumor-bone interface compared to the tumor alone area in all three cell lines used. The values are mean ± SEM. This is a representative of three experiments with similar results

with increased osteolysis and numbers of activated osteoclasts, suggesting that tumor–stromal interactions regulate RANKL-mediated osteoclast activation and tumor-induced osteolysis.

A major barrier to progress in identifying the molecular mechanism(s) of osteolytic breast cancer bone metastasis is the lack of appropriate animal models that fully reflect the biology of human breast cancer metastasis to bone [35, 36]. These models of human bone metastasis of breast cancer produce mixed osteolytic lesions which make it difficult to examine the tumor–stromal interactions. In this study, we used a bone invasion model that mimics the osteolytic changes associated with human cancer [12, 18, 20]. This model allows focused study of the molecular mechanisms governing osteolysis by creating a distinct TB-interface. We used three murine mammary tumor cell lines 4T1, Cl66 and Cl66M2, which are derived from a spontaneous mammary carcinoma in a BALB/c mouse and that exhibit different patterns of spontaneous and experimental lung metastasis [23, 37]. While these three cell lines demonstrate markedly different metastatic potential, we found that each of the three cell lines establish osteolytic lesions in bone when directly implanted and do not differ in their osteolytic potential.

The importance of RANKL signaling at the tumor-bone interface remains unclear [12]. Suppression of the RANKL-RANK signaling axis abrogates both tumor-induced osteolysis and osteolysis associated with arthritis [13–17]. However, little is known about the relative importance of the soluble form of RANKL (sRANKL) in tumor-induced osteolysis. Both MMP7 and Cathepsin G have been shown to be capable of shedding the extracellular domain of RANKL, generating active sRANKL that is capable of inducing widespread osteoclast

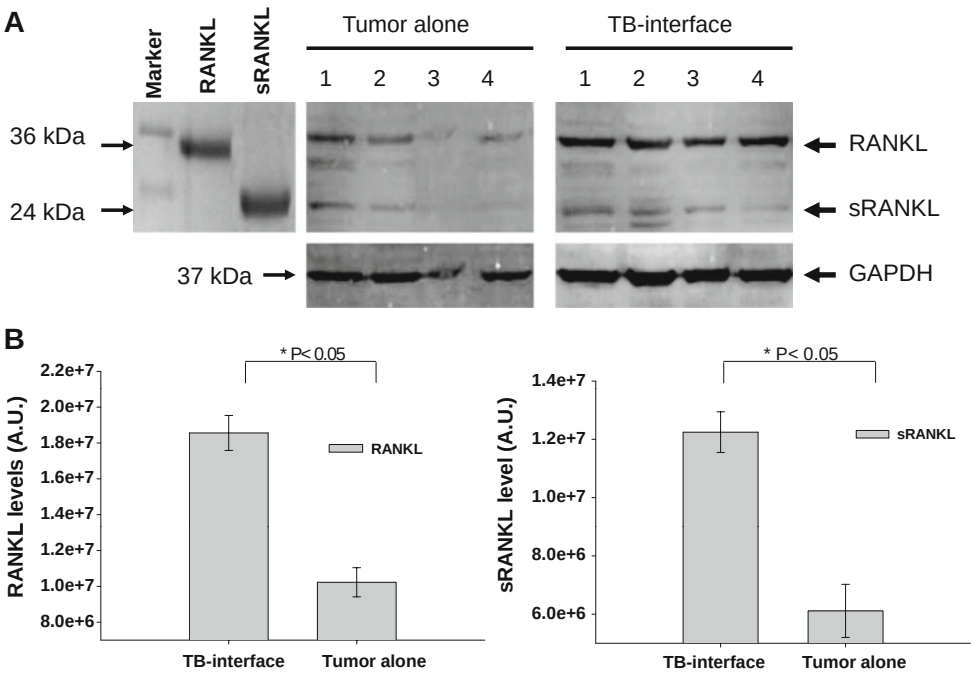

Fig. 4 RANKL and sRANKL proteins during tumor-induced osteolysis. **A** Tissue lysates from tumor alone areas and TB-interface from four different mice (indicated as 1,2,3 and 4) bearing Cl66 tumors were examined for RANKL and sRANKL levels using Western blot analysis. The antibody used in the analysis detects ~36 kDa (membrane bound RANKL) and ~24 kDa (sRANKL). **B** Quantitation of the levels of RANKL and sRANKL was performed using ImageQuant analysis software (GE Biosciences). The levels of RANKL and sRANKL were determined as presented as arbitrary units (A.U.). The values are mean ± SEM. This is a representative of three experiments with similar results

activation [18, 19]. Both RANKL and RANK are membrane-bound proteins and thus require cell to cell contact between RANKL-expressing cells and RANK-expressing cells in order to initiate signaling. Thus, osteoclast activation via RANK activation is limited spatially to the area surrounding RANKL-expressing cells. The significance of the generation of sRANKL lies in the ability to bypass this cell-cell contact requirement and trigger widespread osteoclast activation without any spatial limitation. Accordingly, in these models, inhibition of MMP7 or Cathepsin G significantly reduced tumor-induced osteolysis providing indirect evidence for the importance of sRANKL [18–20]. For the first time, we demonstrate that sRANKL is upregulated at the TB-interface of mammary tumor-induced osteolytic lesions. Importantly, we did not observe a concomitant increase in OPG levels at the tumor-bone interface. Furthermore, the elevated RANKL:OPG ratio that we observed at the tumor-bone interface suggests that not only is there an elevation in absolute RANKL levels but there is also an elevation in the level of free, functional sRANKL that is capable of binding to RANK yielding osteoclast differentiation and activation.

Inhibition of RANKL expression using RANKL-ASO inhibited tumor-induced osteolysis demonstrating the centrality of RANKL signaling in mammary tumor-induced osteolysis. RANKL levels were significantly reduced at the TB-interface of RANKL-ASO treated mice. Interestingly, OPG levels were increased at the TB-interface in these mice. The combination of decreased RANKL expression at the TB-interface and increased OPG led to a significantly decreased RANKL:OPG ratio. Previous studies have suggested the importance of the sRANKL:OPG ratio in serum as a prognostic indicator in osteolytic bone metastasis [38–41]. Our report suggests that this serum prognostic factor is likely a reflection of what is occurring in the bone microenvironment at the TB-interface.

Studies in the animal model of bone metastasis suggest that malignant breast cancer cells and clinical data demonstrate that bone resorption is associated with progression of bone metastases [2, 5, 6, 42–45]. Preclinical studies demonstrate that animals pretreated with bisphosphanate prior to bone colonization of breast cancer cells, showed significant reduction in the number and progression of bone metastases [46–48]. However, bisphosphanate treatment in animals with established bone metastasis did not consistently inhibit disease progression, despite a substantial anti-osteolytic effect, which could be due to elimination of bone forming osteoblasts by the tumor cells [46–49], Furthermore, in human patients bisphosphonates have been shown to affect bone density, but not overall survival of breast cancer patients [44, 50, 51]. These studies suggest that the vicious cycle might be critical for initial steps during bone metastasis and later on malignant cells become independent of bone-derived growth factors [48]. Therefore, novel therapeutic strategies to prevent and treat breast cancer bone metastases are required.

In summary, the present study demonstrated the importance of RANKL signaling at the TB-interface of mammary tumor-induced osteolytic lesions, supporting

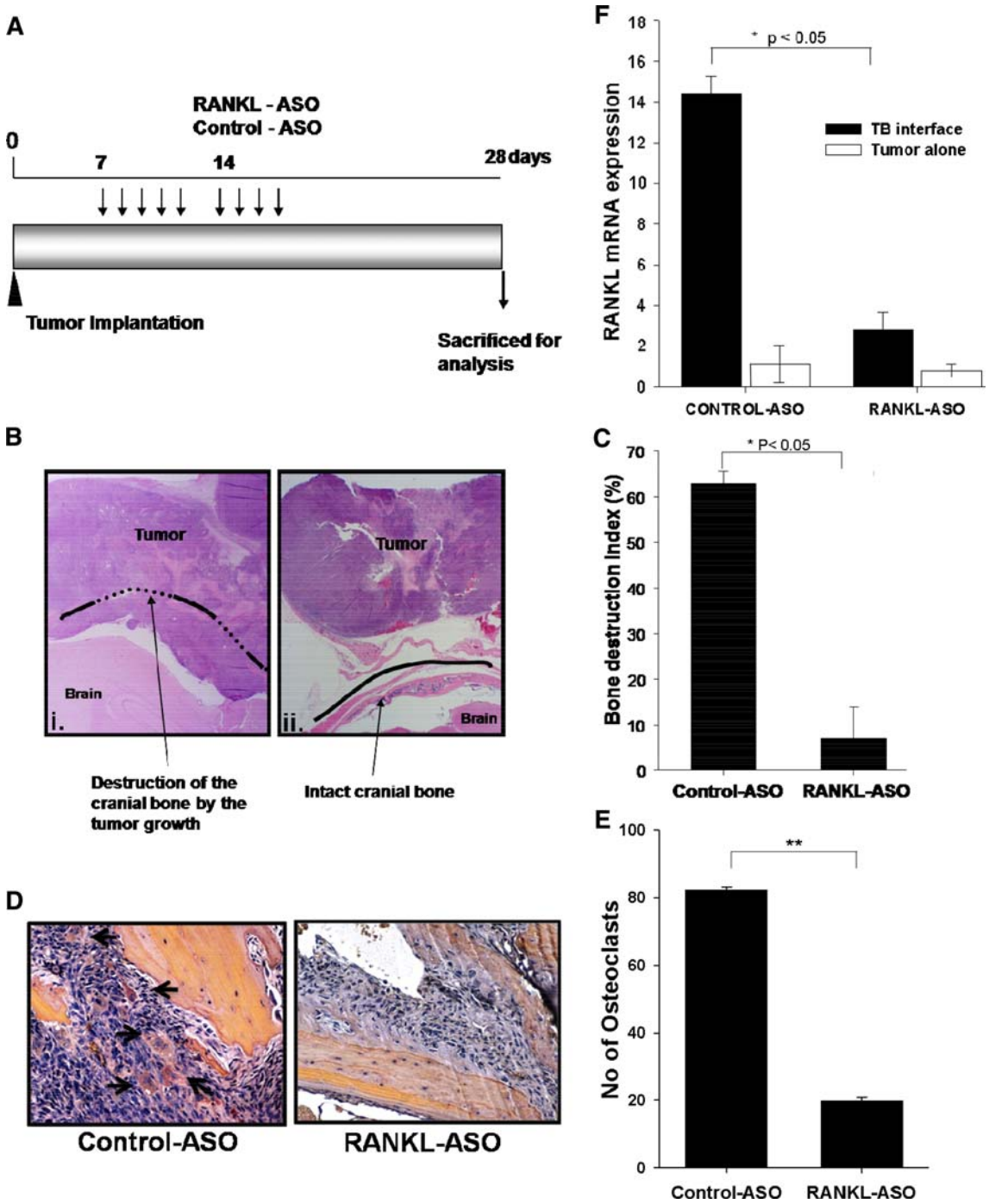

Fig. 5 Inhibition of RANKL expression abrogated tumor-induced osteolysis. **A** Experimental strategy for treatment of Cl66 tumor bearing mice with RANKL-ASO and control-ASO. **B** H&E-stained section (20× magnification) of tumors from control-ASO (**i**) and RANKL-ASO (**ii**) treated animals. *Solid line* represents intact bone and the dotted line shows the osteolytic lesion induced by the tumor. **C** The bone destruction index was significantly reduced in RANKL-ASO treated animals compared to control-ASO treated animals. **F** qRT-PCR demonstrated that RANKL mRNA expression was significantly reduced at the tumor-bone interface of RANKL-ASO treated animals demonstrating the efficacy of the RANKL-ASO. **D**, **E** Number of TRAP positive osteoclasts in RANKL-ASO and control treated animals. The values are mean ± SEM. This is a representative of three experiments with similar results.

previous studies [12, 14–16]. In addition, our data demonstrated increased sRANKL generation at the TB-interface and suggested that the RANKL:OPG ratio is positively associated with the degree of osteolysis. Together, these results demonstrated that not only upregulation of RANKL but also generation of sRANKL at the TB-interface is an important mediator of RANKL-dependent tumor-induced osteolysis.

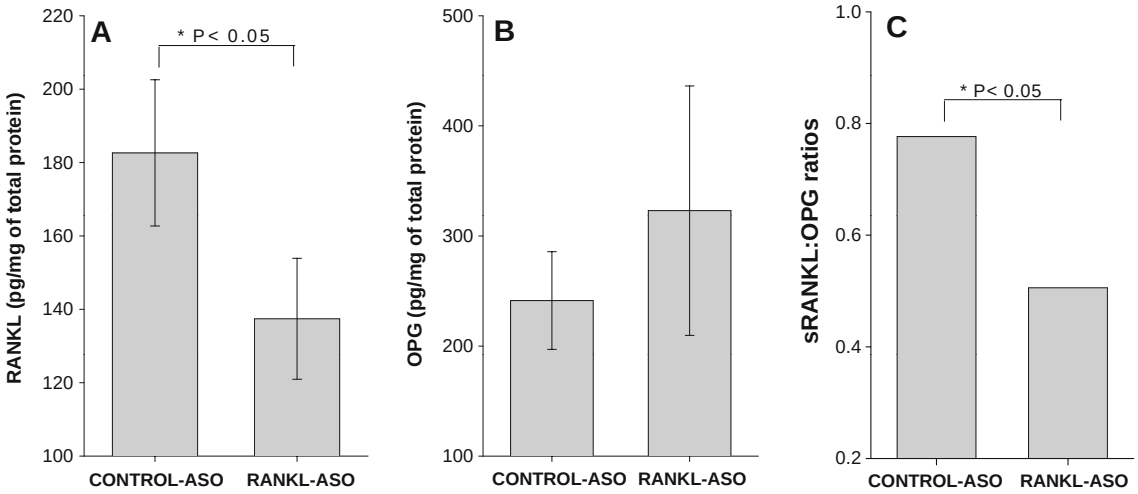

Fig. 6 Inhibiting RANKL expression regulates RANKL and OPG production at the TB interface. RANKL levels at the TB-interface of RANKL-ASO treated animals were significantly reduced compared to control-ASO animals. Five mice were used in each group and the experiment was repeated twice. **A** While OPG levels were concomitantly increased (but not significantly different) in RANKL-ASO treated animals (**B**) as demonstrated by ELISA. **C** The RANKL:OPG ratio was decreased significantly at the tumor-bone interface of RANKL-ASO treated animals compared to control-ASO treated animals. The values are mean ± SEM. This is a representative of three experiments with similar results

Acknowledgments This work was supported in part by grants CA72781 (R.K.S.) and Cancer Center Support Grant (P30CA036727) from National Cancer Institute, National Institutes of Health, Susan G. Komen for the Cure grant KG090860 and Nebraska Research Initiative Program in Cancer Glycobiology (R.K.S.), Department of Defense Breast Cancer Research Program Predoctoral traineeship award (K.C.N) and the Howard Hughes Medical Institute Research Training Fellowship (T.J.W.). We thank Dr. James Eudy and the UNMC DNA Microarray Core Facility for help in microarray analysis.

References

1. Jemal A, Siegel R, Ward E, Hao Y, Xu J, Murray T et al (2008) Cancer statistics, 2008. CA Cancer J Clin 58(2):71–96
2. Mundy GR (2002) Metastasis to bone: causes, consequences and therapeutic opportunities. Nat Rev Cancer 2(8):584–593
3. Boyce BF, Yoneda T, Guise TA (1999) Factors regulating the growth of metastatic cancer in bone. Endocr Relat Cancer 6(3):333–347
4. Coleman RE (1997) Skeletal complications of malignancy. Cancer 80(8 Suppl):1588–1594
5. Kakonen SM, Mundy GR (2003) Mechanisms of osteolytic bone metastases in breast carcinoma. Cancer 97(3 Suppl):834–839
6. Roodman GD (2004) Mechanisms of bone metastasis. N Engl J Med 350(16):1655–1664
7. Lacey DL, Tan HL, Lu J, Kaufman S, Van G, Qiu W et al (2000) Osteoprotegerin ligand modulates murine osteoclast survival in vitro and in vivo. Am J Pathol 157(2):435–448
8. Dougall WC, Chaisson M (2006) The RANK/RANKL/OPG triad in cancer-induced bone diseases. Cancer Metastasis Rev 25(4):541–549
9. Morrissey C, Kostenuik P, Brown L, Vessella R, Corey E (2007) Host-derived RANKL is responsible for osteolysis in a C4-2 human prostate cancer xenograft model of experimental bone metastases. BMC Cancer 7(1):148
10. Dallas SL, Rosser JL, Mundy GR, Bonewald LF (2002) Proteolysis of latent transforming growth factor-beta (TGF-beta)-binding protein-1 by osteoclasts. A cellular mechanism for release of TGF-beta from bone matrix. J Biol Chem 277(24): 21352–21360
11. Lacey DL, Timms E, Tan H-L, Kelley MJ, Dunstan CR, Burgess T et al (1998) Osteoprotegerin ligand is a cytokine that regulates osteoclast differentiation and activation. Cell 93(2):165–176
12. Kitazawa S, Kitazawa R (2002) RANK ligand is a prerequisite for cancer-associated osteolytic lesions. J Pathol 198(2):228–236
13. Tanaka S, Nakamura K, Takahasi N, Suda T (2005) Role of RANKL in physiological and pathological bone resorption and therapeutics targeting the RANKL-RANK signaling system. Immunol Rev 208:30–49
14. Roodman GD, Dougall WC (2008) RANK ligand as a therapeutic target for bone metastases and multiple myeloma. Cancer Treat Rev 34(1):92–101
15. Zhang J, Dai J, Qi Y, Lin DL, Smith P, Strayhorn C et al (2001) Osteoprotegerin inhibits prostate cancer-induced osteoclastogenesis and prevents prostate tumor growth in the bone. J Clin Invest 107(10):1235–1244
16. Zhang J, Dai J, Yao Z, Lu Y, Dougall W, Keller ET (2003) Soluble receptor activator of nuclear factor kappaB Fc diminishes prostate cancer progression in bone. Cancer Res 63(22): 7883–7890
17. Morony S, Capparelli C, Sarosi I, Lacey DL, Dunstan CR, Kostenuik PJ (2001) Osteoprotegerin inhibits osteolysis and decreases skeletal tumor burden in syngeneic and nude mouse models of experimental bone metastasis. Cancer Res 61(11): 4432–4436
18. Wilson TJ, Nannuru KC, Futakuchi M, Sadanandam A, Singh RK (2008) Cathepsin G enhances mammary tumor-induced osteolysis by generating soluble receptor activator of nuclear factor-{kappa}B ligand. Cancer Res 68(14):5803–5811
19. Wilson TJ, Singh RK (2008) Proteases as modulators of tumor–stromal interaction: primary tumors to bone metastases. Biochimica et Biophysica Acta (BBA) Rev Cancer 1785(2):85–95

20. Lynch CC, Hikosaka A, Acuff HB, Martin MD, Kawai N, Singh RK et al (2005) MMP-7 promotes prostate cancer-induced osteolysis via the solubilization of RANKL. Cancer Cell 7(5):485–496
21. Chesneau V, Becherer JD, Zheng Y, Erdjument-Bromage H, Tempst P, Blobel CP (2003) Catalytic properties of ADAM19. J Biol Chem 278(25):22331–22340
22. Schlondorff J, Lum L, Blobel CP (2001) Biochemical and pharmacological criteria define two shedding activities for TRANCE/OPGL that are distinct from the tumor necrosis factor alpha convertase. J Biol Chem 276(18):14665–14674
23. Aslakson CJ, Miller FR (1992) Selective events in the metastatic process defined by analysis of the sequential dissemination of subpopulations of a mouse mammary tumor. Cancer Res 52(6): 1399–1405
24. Chen Z, Varney ML, Backora MW, Cowan K, Solheim JC, Talmadge JE et al (2005) Down-regulation of vascular endothelial cell growth factor-C expression using small interfering RNA vectors in mammary tumors inhibits tumor lymphangiogenesis and spontaneous metastasis and enhances survival. Cancer Res 65(19):9004–9011
25. Heppner GH, Miller FR, Shekhar PM (2000) Nontransgenic models of breast cancer. Breast Cancer Res 2(5):331–334
26. Huang X, Wong MK, Yi H, Watkins S, Laird AD, Wolf SF et al (2002) Combined therapy of local and metastatic 4T1 breast tumor in mice using SU6668, an inhibitor of angiogenic receptor tyrosine kinases, and the immunostimulator B7.2-IgG fusion protein. Cancer Res 62(20):5727–5735
27. Lelekakis M, Moseley JM, Martin TJ, Hards D, Williams E, Ho P et al (1999) A novel orthotopic model of breast cancer metastasis to bone. Clin Exp Metastasis 17(2):163–170
28. Murphy BO, Joshi S, Kessinger A, Reed E, Sharp JG (2002) A murine model of bone marrow micrometastasis in breast cancer. Clin Exp Metastasis 19(7):561–569
29. Sloan EK, Stanley KL, Anderson RL (2004) Caveolin-1 inhibits breast cancer growth and metastasis. Oncogene 23(47):7893–7897
30. Bennett CF, Cowsert LM (1999) Antisense oligonucleotides as a tool for gene functionalization and target validation. Biochim Biophys Acta 1489(1):19–30
31. Henry SP, Geary RS, Yu R, Levin AA (2001) Drug properties of second-generation antisense oligonucleotides: how do they measure up to their predecessors? Curr Opin Invest Drugs 2(10): 1444–1449
32. Kingsley LA, Fournier PGJ, Chirgwin JM, Guise TA (2007) Molecular biology of bone metastasis. Mol Cancer Ther 6(10): 2609–2617
33. Siclari VA, Guise TA, Chirgwin JM (2006) Molecular interactions between breast cancer cells and the bone microenvironment drive skeletal metastases. Cancer Metastasis Rev 25(4):621–633
34. Blair JM, Zhou H, Seibel MJ, Dunstan CR (2006) Mechanisms of disease: roles of OPG, RANKL and RANK in the pathophysiology of skeletal metastasis. Nat Clin Pract Oncol 3(1):41–49
35. Kuperwasser C, Dessain S, Bierbaum BE, Garnet D, Sperandio K, Gauvin GP et al (2005) A mouse model of human breast cancer metastasis to human bone. Cancer Res 65(14):6130–6138
36. Reddi AH, Roodman D, Freeman C, Mohla S (2003) Mechanisms of tumor metastasis to the bone: challenges and opportunities. J Bone Miner Res 18(2):190–194
37. Varney ML, Singh S, Backora M, Chen Z, Singh RK (2008) Lymphangiogenesis and anti-tumor immune responses. Curr Mol Med (In Press)
38. Grimaud E, Soubigou L, Couillaud S, Coipeau P, Moreau A, Passuti N et al (2003) Receptor activator of nuclear factor kappaB ligand (RANKL)/osteoprotegerin (OPG) ratio is increased in severe osteolysis. Am J Pathol 163(5):2021–2031
39. Jung K, Stephan C, Semjonow A, Lein M, Schnorr D, Loening SA (2003) Serum osteoprotegerin and receptor activator of nuclear factor-kappa B ligand as indicators of disturbed osteoclastogenesis in patients with prostate cancer. J Urol 170(6 Pt 1): 2302–2305
40. Seidel C, Hjertner O, Abildgaard N, Heickendorff L, Hjorth M, Westin J et al (2001) Serum osteoprotegerin levels are reduced in patients with multiple myeloma with lytic bone disease. Blood 98(7):2269–2271
41. Terpos E, Szydlo R, Apperley JF, Hatjiharissi E, Politou M, Meletis J et al (2003) Soluble receptor activator of nuclear factor kappaB ligand-osteoprotegerin ratio predicts survival in multiple myeloma: proposal for a novel prognostic index. Blood 102(3): 1064–1069
42. Kostenuik PJ, Singh G, Suyama KL, Orr FW (1992) Stimulation of bone resorption results in a selective increase in the growth rate of spontaneously metastatic Walker 256 cancer cells in bone. Clin Exp Metastasis 10(6):411–418
43. Schneider A, Kalikin LM, Mattos AC, Keller ET, Allen MJ, Pienta KJ et al (2005) Bone turnover mediates preferential localization of prostate cancer in the skeleton. Endocrinology 146(4):1727–1736
44. Brown JE, Cook RJ, Major P, Lipton A, Saad F, Smith M et al (2005) Bone turnover markers as predictors of skeletal complications in prostate cancer, lung cancer, and other solid tumors. JNCI J Natl Cancer Inst 97(1):59–69
45. Costa L, Demers LM, Gouveia-Oliveira A, Schaller J, Costa EB, de Moura MC et al (2002) Prospective evaluation of the peptide-bound collagen type I cross-links *N*-telopeptide and C-telopeptide in predicting bone metastases status. J Clin Oncol 20(3):850–856
46. Sasaki A, Boyce BF, Story B, Wright KR, Chapman M, Boyce R et al (1995) Bisphosphonate risedronate reduces metastatic human breast cancer burden in bone in nude mice. Cancer Res 55(16):3551–3557
47. van der Pluijm G, Que I, Sijmons B, Buijs JT, Lowik CWGM, Wetterwald A et al (2005) Interference with the microenvironmental support impairs the de novo formation of bone metastases in vivo. Cancer Res 65(17):7682–7690
48. Buijs JT, Que I, Lowik CW, Papapoulos SE, Van der Pluijm G (2009) Inhibition of bone resorption and growth of breast cancer in the bone microenvironment. Bone 44(2):380–386
49. Phadke PA, Mercer RR, Harms JF, Jia Y, Frost AR, Jewell JL et al (2006) Kinetics of metastatic breast cancer cell trafficking in bone. Clin Cancer Res 12(5):1431–1440
50. Michaelson MD, Smith MR (2005) Bisphosphonates for treatment and prevention of bone metastases. J Clin Oncol 23(32): 8219–8224
51. Saarto T, Vehmanen L, Virkkunen P, Blomqvist C (2004) Ten-year follow-up of a randomized controlled trial of adjuvant clodronate treatment in node-positive breast cancer patients. Acta Oncol 43(7):650–656

Cathepsin G Enhances Mammary Tumor–Induced Osteolysis by Generating Soluble Receptor Activator of Nuclear Factor-κB Ligand

Thomas J. Wilson,[1] Kalyan C. Nannuru,[1] Mitsuru Futakuchi,[2] Anguraj Sadanandam,[1] and Rakesh K. Singh[1]

[1]Department of Pathology and Microbiology, University of Nebraska Medical Center, Omaha, Nebraska and [2]Department of Experimental Pathology and Tumor Biology, Graduate School of Medical Sciences, Nagoya City University, Nagoya, Japan

Abstract

Breast cancer commonly causes osteolytic metastases in bone, a process that is dependent on tumor-stromal interaction. Proteases play an important role in modulating tumor-stromal interactions in a manner that favors tumor establishment and progression. Whereas several studies have examined the role of proteases in modulating the bone microenvironment, little is currently known about their role in tumor-bone interaction during osteolytic metastasis. In cancer-induced osteolytic lesions, cleavage of receptor activator of nuclear factor-κB ligand (RANKL) to a soluble version (sRANKL) is critical for widespread osteoclast activation. Using a mouse model that mimics osteolytic changes associated with breast cancer–induced bone metastases, we identified cathepsin G, cathepsin K, matrix metalloproteinase (MMP)-9, and MMP13 to be proteases that are up-regulated at the tumor-bone interface using comparative cDNA microarray analysis and quantitative reverse transcription-PCR. Moreover, we showed that cathepsin G is capable of shedding the extracellular domain of RANKL, generating active sRANKL that is capable of inducing differentiation and activation of osteoclast precursors. The major source of cathepsin G at the tumor-bone interface seems to be osteoclasts that up-regulate production of cathepsin G via interaction with tumor cells. Furthermore, we showed that *in vitro* osteoclastogenesis is reduced by inhibition of cathepsin G in a coculture model and that *in vivo* inhibition of cathepsin G reduces mammary tumor–induced osteolysis. Together, our data indicate that cathepsin G activity at the tumor-bone interface plays an important role in mammary tumor–induced osteolysis and suggest that cathepsin G is a potentially novel therapeutic target in the treatment of breast cancer bone metastasis. [Cancer Res 2008;68(14):5803–11]

Introduction

As the most common type of cancer in women in the United States and the second leading cause of cancer-related death, breast cancer represents a serious health problem (1). Metastatic disease is responsible for most of breast cancer–related mortality, accounting for the sharp decline in 5-year survival observed as breast cancer progresses from regional to distant metastasis (1). In patients that ultimately succumb to breast cancer, nearly all are found to have bone metastases, showing the tropism of breast cancer cells to bone. These metastatic bone lesions, predominantly osteolytic in nature, carry severe consequences including hypercalcemia, pathologic fracture, and leukoerythroblastic anemia (2). As a result, bone metastasis dramatically increases the risk of mortality as well as significantly reduces the quality of life.

The mechanisms involved in breast cancer–induced osteolytic bone metastases have been extensively studied but remain unclear. As breast cancer cells establish secondary colonies in the bone microenvironment, a vicious cycle ensues (2). Tumor cells secrete soluble factors such as interleukin (IL)-1, IL-8, and parathyroid hormone–related peptide that activate osteoblasts and induce expression of receptor activator of nuclear factor-κB ligand (RANKL). RANKL expressed by osteoblasts can then interact with its receptor (RANK) on the cell surface of osteoclast precursors, leading to osteoclast differentiation and activation. Activated osteoclasts then mediate bone degradation through the release of proteases including matrix metalloproteinases (MMP) and cathepsins. As bone is degraded, sequestered growth factors are released that serve as growth and survival factors as well as chemoattractants for tumor cells, promoting the establishment of bone metastases (2). Thus, tumor-stromal interactions play a significant role in the establishment and regulation of osteolytic bone metastases.

Proteases play a major role in tumor-stromal interactions by modifying the bidirectional communication to favor tumor establishment and growth at both the primary tumor site and metastatic site (3–5). In a prostate cancer model, we have previously shown that MMP7 is capable of cleaving membrane-bound RANKL into a soluble version (sRANKL), which relieves the contact-dependent nature of osteoblast-osteoclast interaction, bypasses the rate-limiting step of the vicious cycle, and enhances osteoclast activation and subsequent osteolysis (6). To date, however, no such mechanism has been described in breast cancer.

In the present study, we examined the patterns of expression of proteases at the tumor-bone interface of mammary tumor–induced osteolytic lesions and investigated their functional significance in modulating RANKL-RANK signaling in osteoclast activation and osteolysis. We identified cathepsin G, cathepsin K, MMP9, and MMP13 to be proteases that are up-regulated at the tumor-bone interface. Moreover, we showed that cathepsin G is capable of shedding the extracellular domain of RANKL, generating active sRANKL that is capable of inducing differentiation and activation of osteoclast precursors. Furthermore, we

Note: Supplementary data for this article are available at Cancer Research Online (http://cancerres.aacrjournals.org/).

T.J. Wilson is a Howard Hughes Medical Institute Research Training Fellow.

Requests for reprints: Rakesh K. Singh, Department of Pathology and Microbiology, University Nebraska Medical Center, 985845 Nebraska Medical Center, Omaha, NE 68198-5845. Phone: 402 559 9949; Fax: 402 559 4077; E-mail: rsingh@unmc.edu.

©2008 American Association for Cancer Research.

doi:10.1158/0008-5472.CAN-07-5889

showed that *in vitro* osteoclastogenesis is reduced by inhibition of cathepsin G in a coculture model and subsequently showed that *in vivo* inhibition of cathepsin G reduces mammary tumor–induced osteolysis. Thus, we have shown for the first time a role for cathepsin G at the tumor-bone interface of mammary tumor–induced osteolytic lesions and have uncovered a potential therapeutic target.

Materials and Methods

Animal model and tissue preparation. 4T1, Cl66, and Cl66M2 murine breast adenocarcinoma cell lines were used in this study. Tumor cells (1×10^5) mixed with growth factor–reduced Matrigel were implanted on the dorsal skin flap over the calvaria of female BALB/c mice. Tumor growth was monitored twice a week. Mice were sacrificed and necropsied for examination of osteolytic lesions at 4 wk postimplantation. At that time, the tumor and the underlying bone were divided into two pieces. One piece was used for separation of the tumor-bone interface from the tumor alone area for further analysis and the other piece was used for histology sections. All studies were done in accordance with the Institutional Animal Use and Care Committee of the University of Nebraska Medical Center. For histologic examination, tissues were fixed with periodate-lysine-paraformaldehyde at 4°C for 48 h. The tissues were then transferred into a decalcification solution (15% EDTA with glycerol, pH 7.4–7.5) for 4 wk. The tissue was then paraffin embedded and processed for further analysis.

Microarray analysis and real-time PCR. Calcified frozen sections were serially sectioned into 10-μm slices. Sections were then microdissected to separate the tumor-bone interface from the tumor alone area (Fig. 1*A*). Total RNA was extracted from both the tumor-bone interface and the tumor alone area and then amplified by using a probe amplification kit (Affymetrix). Genetic expression at the tumor-bone interface was compared with the tumor alone area using an Affymetrix Mouse Expression Array (430A). Analysis was done using Affymetrix Gene Chip Operating Software to generate raw expression data. A signal log algorithm was used to compare the quantity of a given transcript in two arrays: a baseline array, here the tumor alone area, and an experimental array, here the tumor-bone interface. The signal log ratio is calculated by comparing each probe pair on the experimental array to the corresponding probe pair on the baseline array and then considering the mean of the log ratios of probe pair intensities across the two arrays. The change in transcript level is then expressed as a log 2 ratio. Using this system, a signal log ratio of 1.0 indicates a 2-fold increase at the tumor-bone interface whereas a ratio of −1.0 indicates a 2-fold decrease. For each set of tissue from 4T1, Cl66, and Cl66M2, the fold change at the tumor-bone interface with respect to the tumor alone area was calculated and the genes were ranked from highest to lowest expression.

For real-time quantitative reverse transcription-PCR (RT-PCR) analysis, total RNA was isolated from tissue at the tumor-bone interface and tumor alone area using Trizol reagent (Invitrogen). Five micrograms of total RNA were used for reverse transcription. First-strand cDNA was generated using oligo$(dT)_{18}$ (Fermentas) and Superscript II RT (Invitrogen). Two microliters of the resulting cDNA (1:10 dilution) were used in the real-time reactions with gene-specific primers. The following gene-specific primers were used: cathepsin G, 5′-GAGTCCAGAAGGGCTGAGTG-3′ and 5′-CCTTTCTCGCATTTGGATGT-3′; cathepsin K, 5′-CCAGTGGGAGCTATGGAAGA-3′ and 5′-CTCCAGGTTATGGGCAGAGA-3′; MMP9, 5′-CATTCGCGTGGATAAGGAGT-3′ and 5′-TCACACGCCAGAAGAATTTG-3′; MMP12, 5′-AATGGGCAACTGGACAACTC-3′ and 5′-ACCGCTTCATCCATCTTGAC-3′; MMP13, 5′-TCCCTGCCCCTTCCCTATGG-3′ and 5′-CTCGGAGCCTGTCAACTGTGG-3′; and glyceraldehyde-3-phosphate dehydrogenase (GAPDH), 5′-AGCCTCGTCCCGTAGACAAAA-3′ and 5′-GATGACAAGCTTCCCATCTCG-3′. Quantitative RT-PCR reactions were carried out with FastStart SYBR Green Master mix (Roche) and MyIQ iCycler (Bio-Rad). Fluorescence intensity was measured at the end of each elongation step as a means to evaluate the amount of formed PCR product. GAPDH was used as a reference to normalize the samples.

Generation of RANKL protein. Full-length RANKL cDNA (NM_003701) with an NH_2-terminal His-tag sequence cloned in pReceiver-B01 (GeneCopoeia) plasmid was used to generate RANKL protein using a TnT Quick Coupled Transcription/Translation system (Promega) per manufacturer's protocol using translation grade [^{35}S]methionine (1,175 Ci/mmol at 10 mCi/mL). Two microliters of the reaction mixture were separated on a 12% SDS-polyacrylamide gel and subsequently visualized and photographed with a Typhoon 9410 Variable Mode Imager (GE Healthcare). The resulting translation product was purified with a His-Trap Crude 1-mL column (GE Healthcare) per manufacturer's protocol. The purified protein was then concentrated by using a Centriprep YM-10 spin column (Omicon) and quantified with the BCA Protein Assay kit per manufacturer's protocol (Pierce).

Protease function assays. To test the activity of each of the proteases, colorimetric substrates were used. One hundred nanograms of cathepsin G or cathepsin K were incubated with 500 μmol/L Suc-AAPF-pNA substrate (Biomol International) in enough buffer to make a 50-μL reaction. The 10× buffer contained 100 mmol/L $CaCl_2$, 500 mmol/L HEPES, 10 mmol/L DTNB, and 0.5% Brij-35. Similar reactions were done for MMP9 and MMP13 with chromogenic MMP substrate (Biomol International). Reaction mixtures were incubated at 37°C for 60 min. Readings were taken on a BioTek ELx800 microplate reader every 15 min at 405 nm.

Protease-mediated cleavage of RANKL. Three micrograms of full-length RANKL were incubated overnight at 37°C alone or with 100 ng of cathepsin G, cathepsin K, MMP9, or MMP13 in enough buffer to make a 25-μL reaction. Reactions were terminated by adding EDTA to a final concentration of 10 mmol/L. The reaction mixture was then separated on a 12% SDS-polyacrylamide gel. The gel was then stained with 0.025% Coomassie brilliant blue (Bio-Rad) and photographed by using a Multi-Image Light Cabinet (Alpha Innotech Corporation). Cathepsin G inhibition was tested by adding Na-Tosyl-Phe-chloromethylketone (TPCK; Sigma-Aldrich) at a final concentration of 1 mmol/L. TPCK was incubated with enzyme and buffer for 30 min at 37°C before adding RANKL. The reaction mixture was then incubated, separated, and analyzed.

Similar reactions were carried out and subsequently used for Western blot analysis. Reaction mixtures were separated on a 12% SDS-polyacrylamide gel and then transferred onto a polyvinylidene difluoride (PVDF) membrane (GE Healthcare) at 100 V for 1 h. The membrane was then washed with 0.1% Tween-TBS. The membrane was then blocked overnight in 5% bovine serum albumin in PBS. The next day, the membrane was incubated for 90 min with 1:500 anti-RANKL antibody that recognizes an epitope near the COOH terminus of RANKL (Santa Cruz Biotechnology) diluted in 0.1% Tween-TBS. After washing in 0.1% Tween-TBS, the membrane was incubated for 60 min with 1:1,500 antigoat-horseradish peroxidase diluted in 0.1% Tween-TBS. Finally, after washing with 0.1% Tween-TBS, the membrane was developed with an enhanced chemiluminescence (ECL) Plus Western Blotting Detection System (GE Healthcare) per manufacturer's protocol and imaged with a Typhoon 9410 Variable Mode Imager (GE Healthcare).

Osteoclast differentiation and activation assay. RAW 264.7 cells were seeded onto eight-well chambered slides at a density of 3,000 per chamber. Cells were grown in DMEM plus 10% fetal bovine serum (FBS), 1% vitamins, 1% L-glutamine, and 0.08% gentamicin (DMEM complete medium). The cells were incubated overnight at 37°C. The following day, the medium was changed and the cells were treated with medium alone, 50 ng/mL sRANKL, or 50 ng/mL cathepsin G–generated sRANKL. The cells were then allowed to incubate for 7 d with medium changes every other day. On the 7th day, cells were stained for tartrate-resistant acid phosphatase (TRAP) per manufacturer's protocol (Sigma-Aldrich). The number of osteoclasts per 250-μm field was counted for five fields per treatment per replicate. Fully mature, TRAP-positive multinucleated cells were counted as osteoclasts.

BD BioCoat Osteologic Coverslips (BD Biosciences) were placed in 24-well plates. RAW 264.7 cells were then seeded onto the plates at a density of 5,000/cm^2. Cells were grown in DMEM complete medium. The cells were incubated overnight at 37°C. The following day, the medium was changed and the cells were treated with medium alone, 50 ng/mL sRANKL, or

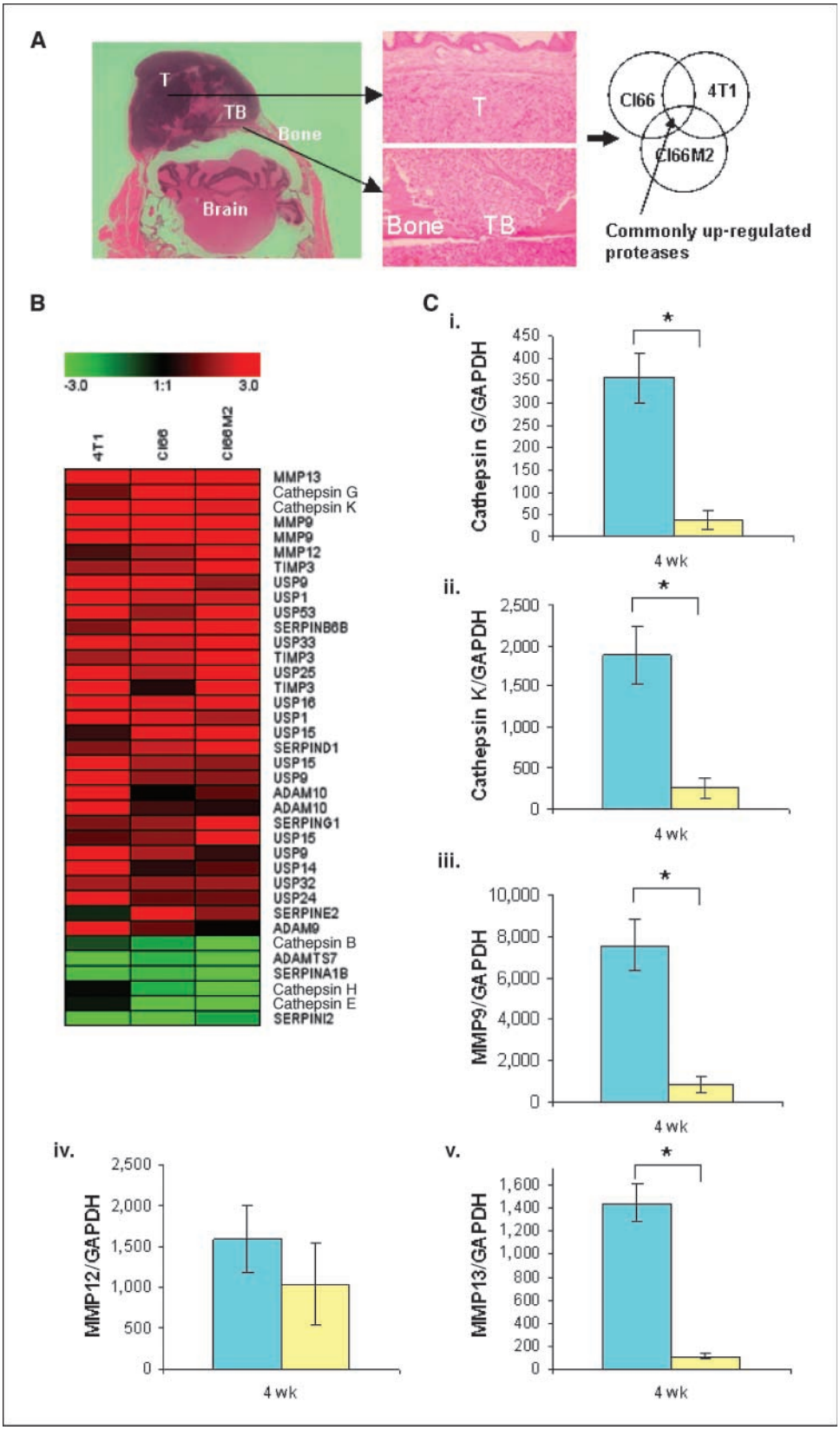

Figure 1. Protease gene expression at the tumor-bone interface. *A,* H&E-stained section of tumor-bone interface (*TB*) and tumor alone (*T*) area. Tumors (Cl66, Cl66M2, and 4T1) were microdissected to separate the tumor alone area from the tumor-bone interface (n = 3). Total RNA and protein were collected from these two regions of the lesions to determine what proteases are up-regulated as tumor cells engage in bidirectional communication with the bone microenvironment. *B,* gene expression at the tumor-bone interface was compared with the tumor alone area by comparative cDNA microarray analysis using week 4 samples from Cl66, Cl66M2, and 4T1 tumors. Protease-specific analysis of the data was conducted. *C, i* to *v,* expression of cathepsin G, cathepsin K, MMP9, MMP12, and MMP13 was confirmed by real-time PCR. *Columns,* average mRNA expression of the specific gene normalized to GAPDH. *Blue columns,* tumor-bone interface; *yellow columns,* tumor alone area. Representative data of all three cell lines done in triplicate. *Bars,* SD. *, $P < 0.05$.

50 ng/mL cathepsin G–generated sRANKL. The cells were then allowed to incubate for 7 d with medium changes every other day. On the 7th day, the medium was aspirated and 1 mL of bleach was added to each well. After 5 min, the bleach was aspirated and the coverslips were washed thrice with distilled water. The coverslips were then stained with hematoxylin for 2 min and then rinsed with running tap water for 10 min. Finally, the number and area of calcium phosphate matrix resorption pits (clear areas) on each 12-mm coverslip were measured.

Immunoblotting for cathepsin G. Fifty micrograms of protein from the tumor-bone interface and tumor alone area for each of the animals injected with Cl66 cells were separated on a 12% SDS-polyacrylamide gel and then was transferred onto a PVDF membrane (GE Healthcare). The membranes were immunoblotted with anti–cathepsin G antibody that recognizes an epitope near the NH_2 terminus of cathepsin G (1:200; Santa Cruz Biotechnology) and anti–β-actin antibody (1:2,000; Santa Cruz Biotechnology) and developed with an ECL Plus Western Blotting Detection System (GE Healthcare) per manufacturer's protocol and imaged with a Typhoon 9410 Variable Mode Imager (GE Healthcare). The bands for both cathepsin G and β-actin were then quantified and compared using ImageQuant 5.1 (Molecular Dynamics).

Immunohistochemistry for cathepsin G. For the *in vivo* detection of cathepsin G, sections were deparaffinized and processed for antigen retrieval. Following nonspecific blocking, sections were then incubated with anti–cathepsin G antibody (Santa Cruz Biotechnology; 1:50 dilution) overnight at 4°C. The sections were then washed and subsequently incubated with biotinylated antigoat IgG antibody diluted to 1:500 for 1 h. Sections were then washed and incubated with avidin-biotin complex (Vector Laboratories) for 45 min. Next, the slides were developed with diaminobenzidine tetrahydrochloride substrate (Vector Laboratories) and counterstained with hematoxylin for 30 s. Antigoat IgG was added in lieu of primary antibody as control and no detectable staining was observed in these sections.

Cathepsin G inhibition coculture model. RAW 264.7 cells were seeded at a density of $3{,}000/cm^2$ on gelatin-coated six-well plates in DMEM plus 10% FBS, 1% vitamins, 1% L-glutamine, and 0.08% gentamicin (DMEM complete medium). Following overnight incubation, cells were incubated with DMEM complete medium alone, DMEM complete medium plus 25% (v/v) Cl66-conditioned medium with or without TPCK at a final concentration of 1 mmol/L, TPCK at a final concentration of 1 mmol/L plus commercially available sRANKL at 50 ng/mL, or DMEM complete medium containing Cl66 cells at a density of $3000/cm^2$ with or without TPCK. In the TPCK-treated groups, TPCK was added to a final concentration of 1 mmol/L every 24 h. After 4 d, the coverslips were stained for TRAP per manufacturer's instructions (Sigma-Aldrich) and multinucleated, TRAP-positive osteoclasts were counted.

***In vivo* inhibition of cathepsin G.** Cl66 tumor cells (1×10^5) mixed with growth factor–reduced Matrigel were implanted on the dorsal skin flap over the calvaria of female BALB/c mice. Tumor growth was monitored twice a week. Beginning 7 d after tumor implantation, mice were injected s.c. with TPCK (Sigma-Aldrich) at 50 mg/kg/d (n = 6) or 50-μL DMSO as control (n = 6) for 21 d. Mice were sacrificed at day 31 postimplantation and necropsied for examination of osteolytic lesions. To calculate the bone destruction index, sections were stained with H&E. The bone destruction index was calculated by dividing the length of bone destruction by the length of the tumor-bone interface and multiplying by 100. All studies were done in accordance with the Institutional Animal Use and Care Committee of the University of Nebraska Medical Center.

Statistical analysis. For *in vivo* studies, the Wilcoxon signed rank test was used to analyze data. For *in vitro* studies, the Student t test was used. $P < 0.05$ was considered significant.

Results

Protease gene expression at the tumor-bone interface. Mammary tumor cells with different metastatic potentials, 4T1 (high), Cl66 (moderate), and Cl66M2 (low), were transplanted into the calvaria of BALB/c mice. Histochemical analysis showed that all tumors exhibited tumor-induced osteolysis and osteoclast activation similar to that observed in breast cancer bone metastasis. Using cDNA microarray analysis, we examined the gene expression patterns at the tumor-bone interface compared with the tumor alone area (Fig. 1*A*). A whole-genome microarray was used and subsequently analyzed by sorting out proteases and protease inhibitors. The five most up-regulated protease genes were *cathepsin G, cathepsin K, MMP9, MMP12*, and *MMP13* (Fig. 1*B*). The common up-regulation of these five genes in all three cell lines further suggested that they may play an important role at the tumor-bone interface.

We then used quantitative RT-PCR to confirm the up-regulation of these five genes at the tumor-bone interface. We confirmed the up-regulation of cathepsin G (Fig. 1*C-i*), cathepsin K (Fig. 1*C-ii*), MMP9 (Fig. 1*C-iii*), and MMP13 (Fig. 1*C-v*), but not MMP12 (Fig. 1*C-iv*), at the tumor-bone interface.

Cathepsin G cleaves RANKL to generate sRANKL. We previously reported that MMP7 plays a role in prostate tumor–induced osteolysis through the cleavage of cell-surface RANKL into a soluble form of RANKL that is capable of enhancing osteoclast differentiation and subsequent osteolysis (6). To determine if any of the proteases that we observed to be up-regulated at the tumor-bone interface play a similar role in mammary tumor–induced osteolysis, the activity of each protease against full-length RANKL was assessed.

Full-length RANKL protein was generated by using an *in vitro* transcription/translation kit. The product was visualized and the expected ~34-kDa protein was seen (Fig. 2*B*). Although activity against the native substrate of each protease was observed (Fig. 2*A-i*), only cathepsin G generated a soluble version of RANKL (~24 kDa; Fig. 2*C*). To confirm cathepsin G–mediated cleavage of RANKL, we used TPCK, a cathepsin G inhibitor, before incubation with full-length RANKL protein. TPCK is an inhibitor of the chymotrypsin-like group of proteases and is a potent inhibitor of cathepsin G (7, 8). We first confirmed the ability of TPCK to inhibit cathepsin G activity against its native substrate, and TPCK effectively inhibited cathepsin G activity (Fig. 2*A-ii*). Similarly, cathepsin G preincubated with TPCK did not cleave RANKL (Fig. 2*D-ii*). Finally, Western blot analysis with an anti-RANKL antibody that recognizes an epitope near the COOH terminus confirmed that the cleaved protein was RANKL and that the soluble product generated was derived from full-length RANKL cleaved near the NH_2 terminus within the extracellular domain (Fig. 2*D-i*).

Cathepsin G–generated sRANKL induces osteoclast differentiation and activation. The ability of cathepsin G–generated sRANKL to induce osteoclast differentiation and activation was assessed using the murine monocyte/macrophage cell line RAW 264.7. Fully mature, TRAP-positive multinucleated cells were counted as osteoclasts (Fig. 3*B-ii*). Commercially available sRANKL (positive control) induced significantly higher osteoclast differentiation than medium alone (negative control; Fig. 3*A*). Numerous TRAP-positive cells were seen in the control sample but most were mononuclear (Fig. 3*B-i*). Similar to the commercial sRANKL, cathepsin G–generated sRANKL induced significantly higher osteoclast formation than control (Fig. 3*A*). Although osteoclast differentiation was higher in the sRANKL-treated group, it did not differ statistically from the cathepsin G–generated sRANKL–treated group.

We then examined whether or not the osteoclasts produced by treatment with cathepsin G–generated sRANKL are active. Osteoclast activation was assessed by counting the number of calcium phosphate matrix resorption pits formed per BD BioCoat Osteologic Coverslip. Commercially available sRANKL (positive control) induced activation of osteoclasts with a significantly higher number of resorptive pits compared with medium alone (negative control; Fig. 3*C* and *D*). Similarly, cathepsin G–generated sRANKL yielded a significantly higher number of pits compared

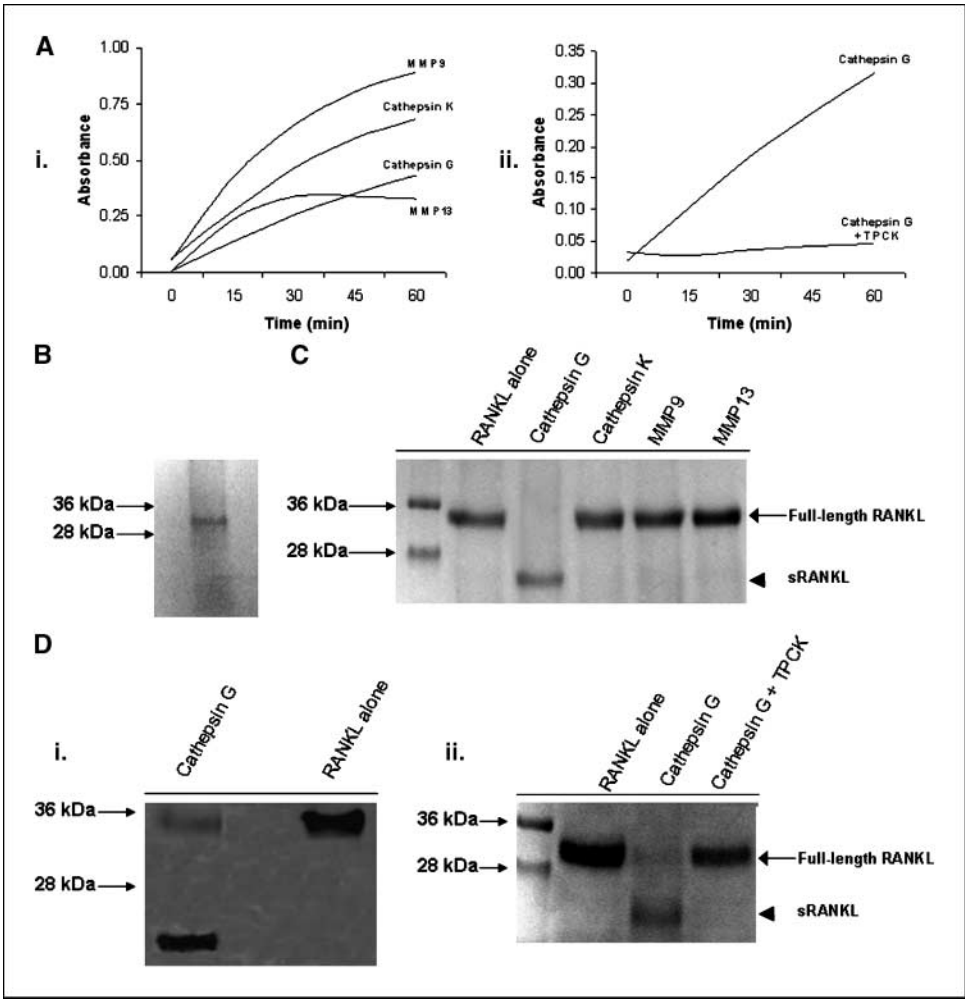

Figure 2. Cathepsin G–dependent generation of sRANKL. *A, i,* the activity of each of the proteases was tested against colorimetric substrates to ensure appropriate reaction conditions. Each of the proteases showed activity against the substrate over a 60-min period. *ii,* TPCK, an inhibitor of cathepsin G, effectively inhibited the action of cathepsin G against the substrate at a concentration of 1 mmol/L. *B,* RANKL was generated by using an *in vitro* transcription/translation kit and then purified. A single band at ~34 kDa is appropriate for RANKL and shows the purity of the sample. *C,* cathepsin G incubated with full-length RANKL (*arrow*) generated a soluble ~24-kDa product (*arrowhead*). *D, i,* Western blot with anti-RANKL antibody directed at an epitope at the COOH terminus confirms that cathepsin G cleaves RANKL near the NH_2 terminus. *ii,* TPCK, a cathepsin G inhibitor, blocked cleavage of RANKL, confirming that cathepsin G is responsible for the generation of sRANKL.

with control and was statistically indistinguishable from commercially available sRANKL (Fig. 3*C* and *D*). Together, these results indicate that cathepsin G–generated sRANKL is capable of inducing osteoclast differentiation and activation and suggest that increased cathepsin G activity at the tumor-bone interface can lead to increased osteoclast differentiation and subsequent osteolysis.

Up-regulation of cathepsin G at the tumor-bone interface. Recognizing that cathepsin G may make a significant contribution to the vicious cycle, we reexamined cathepsin G expression at the tumor-bone interface and further confirmed its up-regulation at the protein level by Western blot analysis comparing the tumor-bone interface to the tumor alone area. Cl66 tumors showed significant up-regulation of cathepsin G at the tumor-bone interface as compared with the tumor alone area (Fig. 4*A* and *B*). This protein level analysis confirmed the earlier cDNA microarray and quantitative RT-PCR analyses.

Osteoclasts/osteoclast precursors are the major source of cathepsin G. To determine the source of cathepsin G at the tumor-bone interface, immunohistochemistry was used to assess the source of cathepsin G *in vivo*. Osteoclasts and osteoclast precursors stained strongly positive for cathepsin G (Fig. 4*C-i*), whereas tumor cells at the tumor-bone interface stained moderately positive (Fig. 4*C-i*). Tumor cells away from the tumor-bone interface in the tumor alone area stained weakly positive (Fig. 4*C-ii*). Normal bone did not show any immunoreactivity to cathepsin G (Fig. 4*C-iii*). These data agree with our *in vitro* data (Supplementary data) that tumor cells have minimal baseline expression of cathepsin G that is up-regulated as they interact with osteoclast precursors, but osteoclasts are the major source of cathepsin G at the tumor-bone interface.

Inhibition of cathepsin G blocks osteoclastogenesis *in vitro*. RAW 264.7 cells treated with 25% Cl66-conditioned medium showed significantly higher osteoclast differentiation compared with control (Fig. 5*A*), suggesting that a soluble factor produced by Cl66 cells is capable of inducing osteoclast differentiation. To determine whether cathepsin G is responsible for the generation of this soluble factor, Cl66 cells were treated with TPCK while collecting conditioned medium. Cl66-conditioned medium from cells treated with TPCK induced significantly lower osteoclast differentiation compared with Cl66-conditioned medium from untreated cells (Fig. 5*A*). Importantly, RAW 264.7 cells treated with both TPCK and sRANKL showed significant osteoclast formation, showing that reduction in osteoclast formation in the TPCK-treated samples is not merely due to death of osteoclasts secondary to TPCK toxicity (Fig. 5*A*). Similarly, RAW 264.7 cells cocultured with Cl66 cells showed significantly higher osteoclast differentiation than RAW 264.7 cells alone (Fig. 5*B*). TPCK also reduced osteoclastogenesis in the coculture but did not eliminate it (Fig. 5*B*). Taken together, these results indicate that cathepsin G is responsible for the generation of a soluble factor capable of

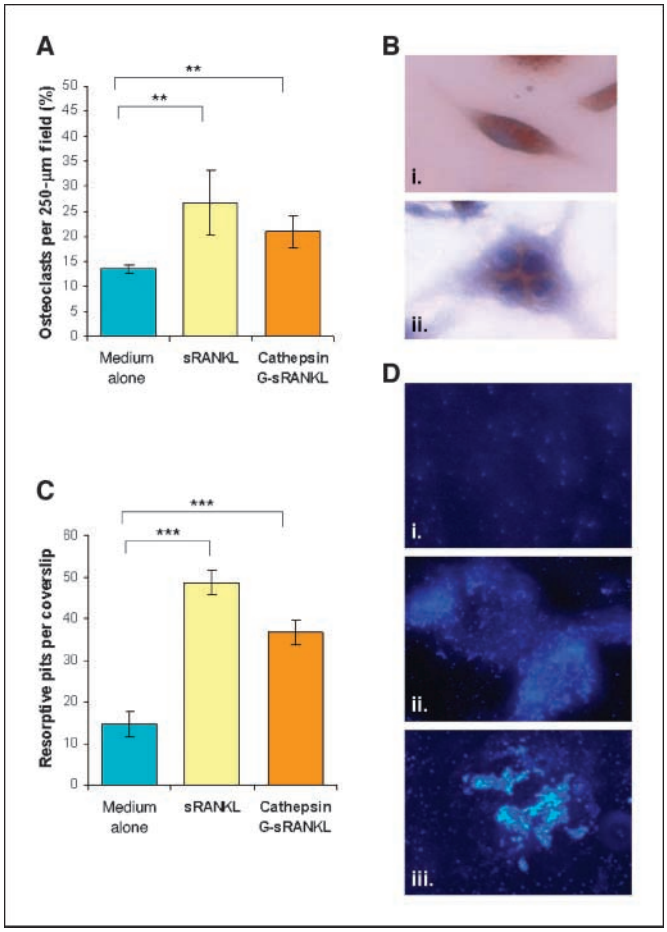

Figure 3. Cathepsin G–generated sRANKL induces osteoclast differentiation and activation. *A,* cathepsin G–generated sRANKL is an active product capable of inducing osteoclast differentiation. RAW 264.7 cells were treated with medium alone (negative control), commercially available sRANKL (positive control), or cathepsin G–generated sRANKL. Cells were stained for TRAP. Fully mature, TRAP-positive multinucleated cells were counted as osteoclasts. The number of osteoclasts per 250-μm field was counted. *Bars,* SD. **, $P < 0.01$ *B, i,* numerous TRAP-positive cells were seen in the medium-alone treatment group but most were mononuclear. *ii,* fully mature, TRAP-positive multinucleated osteoclast typical of sRANKL and cathepsin G–generated sRANKL groups. *C,* RAW 264.7 cells overlaid on coverslips containing artificial bone matrix were treated with medium alone (negative control), commercially available sRANKL (positive control), or cathepsin G–generated sRANKL. The number of calcium phosphate matrix resorption per coverslip was counted. *Bars,* SD. ***, $P < 0.001$. *D, i* to *iii,* typical 250-μm field from medium-alone, sRANKL, and cathepsin G–generated sRANKL groups, respectively. sRANKL and cathepsin G–generated sRANKL induced osteoclast differentiation and activation.

inducing osteoclast differentiation and that inhibition of cathepsin G reduces osteoclast differentiation.

Inhibition of cathepsin G reduces osteolysis *in vivo*. *In vitro* inhibition of cathepsin G reduced osteoclastogenesis, and thus we sought to determine whether inhibition of cathepsin G *in vivo* would reduce mammary tumor–induced osteolysis. No difference was observed in tumor growth or growth kinetics between TPCK-treated mice and negative control mice (data not shown). However, TPCK treatment significantly reduced tumor-induced osteolysis from an average bone destruction index of 35.3% in the DMSO-treated (negative control) mice to 13.2% in the TPCK-treated mice (Fig. 6*A*). Figure 6*B* shows the marked reduction in osteolysis at the tumor-bone interface of TPCK-treated mice compared with the control mice.

Discussion

Proteases play an important role in modulating tumor-stromal interactions in a manner that favors tumor establishment and progression. Although several studies have examined the role of proteases in modulating the bone microenvironment (9–12), little is currently known about their role in tumor-bone interaction during osteolytic metastasis. In this study, we have identified potentially important proteases in mammary tumor–induced osteolytic lesions, including cathepsin G, cathepsin K, MMP9, and MMP13.

Because RANKL is one of the key molecular players in a variety of osteolytic lesions that has previously been shown to be modified by proteases to favor tumor progression (6, 13, 14), we sought to determine if any of the up-regulated proteases were capable of modulating RANKL signaling. The importance of RANKL is in its ability to signal through RANK on preosteoclasts to induce differentiation and activation leading to bone resorption. The rate-limiting step to the vicious cycle is the RANKL-RANK signaling pathway. Because both RANKL and RANK are membrane-bound proteins, this interaction requires physical cell-to-cell contact between osteoblasts and osteoclast precursors in order to occur. Because RANKL, a member of the tumor necrosis factor family of cytokines, stimulates RANK via cell-to-cell contact between osteoblasts and osteoclast precursors, osteoclast differentiation and activation occurs with induction of TRAP activity, calcitonin binding, and actin-ring formation characteristic of osteoclasts (15, 16). The centrality of RANKL to the vicious cycle makes it a molecule that could potentially be up-regulated to establish osteolytic lesions, and in fact, we have found that RANKL is up-regulated at the tumor-bone interface of mammary tumor–induced osteolytic lesions.[3] However, even with up-regulation of RANKL, the number of preosteoclasts that can be activated is spatially limited by their proximity to osteoblasts because cell-cell contact is required. In a prostate cancer model, our group has previously described a mechanism for cleavage of RANKL by MMP7 in a manner that releases it from the cell surface (6). The generation of sRANKL increases the number of preosteoclasts that can be activated and enhances osteolysis. Until now, no such mechanism has been described in mammary tumor–induced osteolytic lesions.

By identifying proteases differentially expressed as a result of tumor-bone interactions, we generated a list of proteases potentially involved in the modulation of RANKL-RANK signaling through the generation of sRANKL. We selected the top five proteases for further evaluation, which included cathepsin G, cathepsin K, MMP9, MMP12, and MMP13. Using quantitative RT-PCR to confirm up-regulation at the tumor-bone interface, we were able to eliminate MMP12 from the list, leaving four up-regulated proteases for further evaluation. Interestingly, RANKL has been shown to induce the expression of both cathepsin K and MMP9 in osteoclast precursor cells (17), and our data agree with this report (data not shown), suggesting that up-regulation of these two proteases may be an effect of enhanced RANKL signaling rather than a cause. Nonetheless, all four proteases were tested for their ability to cleave RANKL. Of these, only cathepsin G was capable of generating sRANKL. Western blot analysis suggests that the cleavage site is near the NH_2 terminus of the RANKL protein because the longer ~24-kDa fragment was detected with an

[3] K.C. Nannuru, M. Futakuchi, A. Sadanandam, T.J. Wilson, M.L. Varney, L.J. Myers, X. Li, E.G. Marcusson, and R.K. Singh. Unpublished data.

anti-RANKL antibody that recognizes an epitope near the COOH terminus. The cleavage site and molecular weight of this larger fragment are similar to those observed in MMP7 cleavage of RANKL (6). Furthermore, the sRANKL generated by cathepsin G is an active product capable of inducing osteoclastogenesis. Osteoclasts are derived from the hematopoietic monocyte/macrophage lineage of cells. For this reason, we used the murine monocyte/macrophage cell line RAW 264.7 to test the activity of cathepsin G–generated sRANKL. Treatment of these cells with cathepsin G–generated sRANKL increased the number of differentiated and activated osteoclasts as shown by an increased number of multinucleated, TRAP-positive cells and the production of resorptive pits when cultured on artificial bone matrix.

The production of sRANKL by cathepsin G circumvents cell-cell contact–dependent signaling between membrane-bound RANKL and RANK, which allows increased osteoclastogenesis and subsequent bone resorption. Thus, cathepsin G can be added to the list of proteases known to be capable of cleaving RANKL, which includes MMP3, MMP7, a disintegrin and metalloproteinase (ADAM)-17, and ADAM19 (6, 18, 19). The generation of sRANKL is one way that cathepsin G may make a significant contribution to the vicious cycle. However, outside of this report, little is currently known about cathepsin G in the pathologic microenvironment of bone metastases.

Although the functional role of cathepsin G is well characterized in a variety of pathologic conditions including rheumatoid arthritis (20), coronary artery disease (21), periodontitis (22), and ischemic reperfusion injury (23), this is the first report of its involvement in bone metastasis. Interestingly, however, the source of cathepsin G in rheumatoid arthritis is macrophages (20). Because osteoclasts are derived from the monocyte/macrophage lineage of cells, this represents a potential source for cathepsin G in the pathologic bone microenvironment. Currently, the other known source of cathepsin G is neutrophils. Cathepsin G is expressed at high levels on the plasma membrane of neutrophils bound to heparin and chondroitin sulfate after neutrophils degranulate (24). Whether or not neutrophils are an important source of cathepsin G at the tumor-bone interface is not currently known.

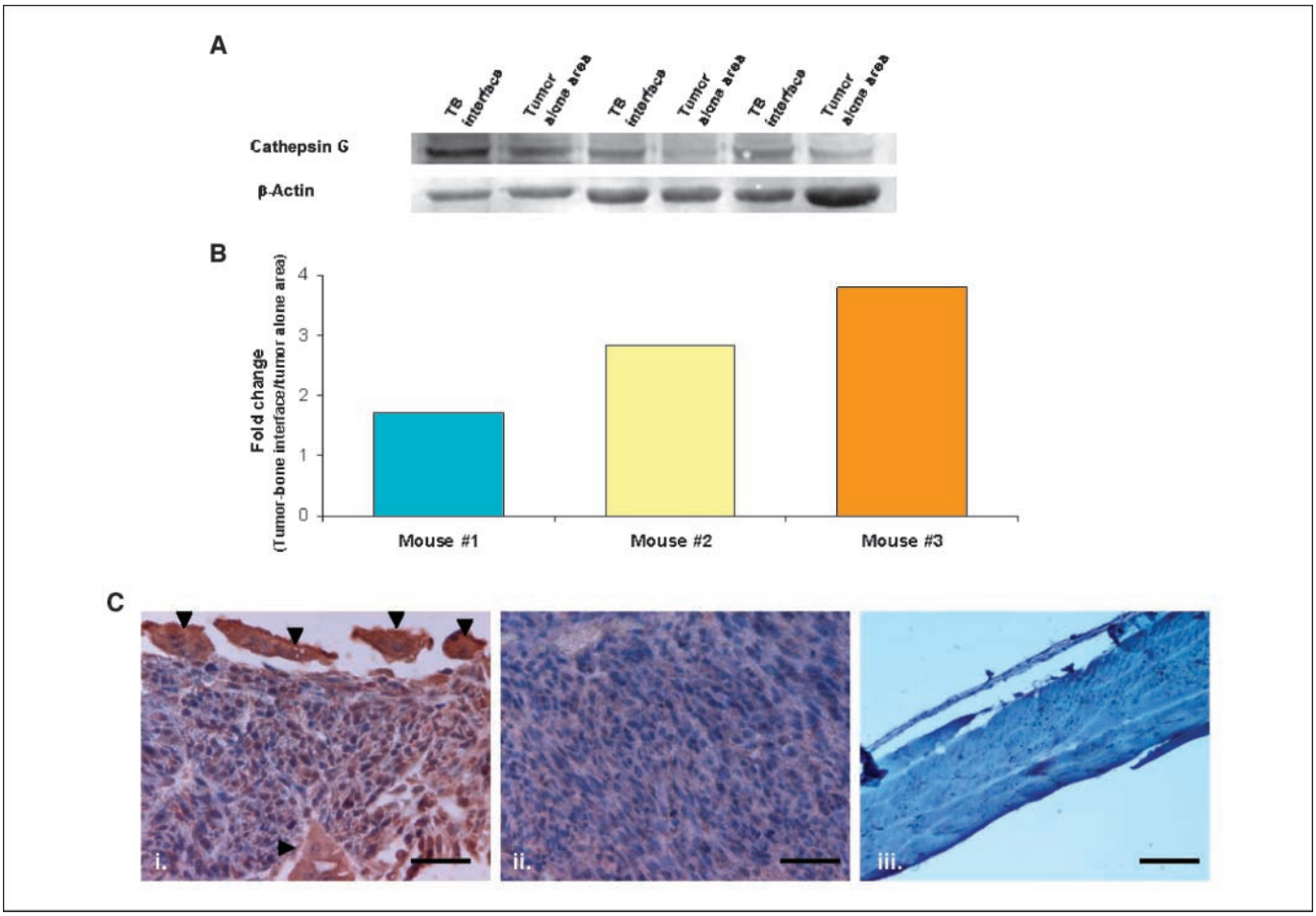

Figure 4. Expression of cathepsin G at the tumor-bone interface. *A,* Western blot analysis was done for mice bearing Cl66 tumors comparing cathepsin G expression at the tumor-bone interface to expression in the tumor alone area. Cathepsin G is up-regulated at the tumor-bone interface compared with the tumor-alone area. *B,* the expression of cathepsin G was quantified using ImageQuant gel analysis software (GE Healthcare). The expression indices for cathepsin G expression at the tumor-bone interface and tumor alone area were calculated by comparing the intensities of the cathepsin G and β-actin bands. The values are fold increase in cathepsin G expression at the tumor-bone area as compared with tumor alone area. Cathepsin G is increased at the tumor-bone interface compared with the tumor alone area in all three mice. *C,* immunohistochemistry for cathepsin G was done on sections from Cl66 tumor–bearing mice and non–tumor-bearing mice. *i,* osteoclasts (*arrowheads*) and osteoclast precursors stained strongly positive for cathepsin G and are the major source at the tumor-bone interface. Tumor cells near the tumor-bone interface stained moderately positive. *ii,* tumor cells in the tumor alone area stained weakly positive for cathepsin G. *iii,* immunostaining of normal bone showing no cathepsin G expression. *Bar,* 0.01 mm.

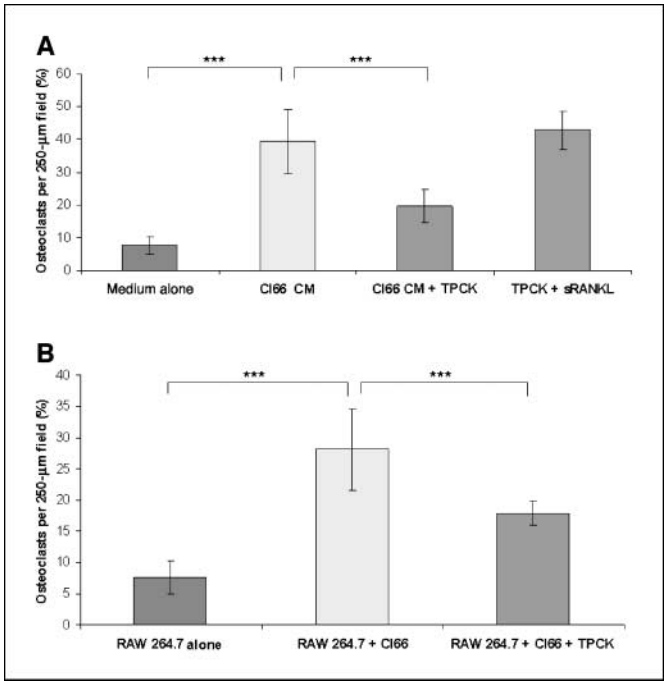

Figure 5. Inhibition of cathepsin G activity abrogates osteoclastogenesis. *A,* Cl66 conditioned medium (*CM*) induced higher osteoclastogenesis in RAW 264.7 cells compared with control (*medium alone*). TPCK treatment during collection of conditioned medium reduced osteoclastogenesis. Cl66 cells treated with TPCK plus commercially available sRANKL also showed higher osteoclastogenesis, showing that TPCK is not toxic to osteoclasts. *B,* Cl66 cells cocultured with RAW 264.7 cells induced higher osteoclastogenesis compared with RAW 264.7 cells alone. TPCK treatment reduced, but did not eliminate, this osteoclastogenesis. ***, $P < 0.001$.

To evaluate the source of cathepsin G in the bone microenvironment, immunohistochemistry was done. These studies supported the *in vitro* conclusion (Supplementary data) that osteoclasts likely make a significant contribution to the observed up-regulation of cathepsin G at the tumor-bone interface. Osteoclasts stained strongly positive for cathepsin G, whereas tumor cells at the tumor-bone interface showed moderate positivity. Osteoclast precursors that interspersed within the tumor cells also stained strongly positive. Further away from the tumor-bone interface in the tumor alone area, positivity for cathepsin G among the tumor cells became weaker and more sparse. Thus, this supports that tumor cells have low, baseline expression of cathepsin G that is up-regulated through interactions with osteoclast precursors but that osteoclasts are the major source of cathepsin G at the tumor-bone interface.

In addition to osteoblasts, all three cell lines (4T1, Cl66, and Cl66M2) used in this study express RANKL as well as cathepsin G (data not shown). The constitutive, low-level expression of cathepsin G by the tumor cells may be a mechanism by which they constitutively produce low levels of sRANKL. Thus, as tumor cells enter the bone microenvironment, they produce low levels of sRANKL, which triggers osteoclast differentiation and increased cathepsin G production. As the production of cathepsin G is then amplified, sRANKL production is increased, osteoclast differentiation is subsequently increased, and sequestered growth factors are released from the bone matrix that favor tumor progression. Thus, we are left with the potential for a new model of the osteolytic vicious cycle in which cathepsin G plays a central role.

Cathepsin G is potentially a central player in the vicious cycle, and thus, it represents an exciting potential therapeutic target in the treatment of mammary tumor–induced osteolysis. To test the effects of cathepsin G inhibition *in vitro*, we used a coculture model. Cl66-conditioned medium induced osteoclastogenesis in RAW 264.7 cells, suggesting that Cl66 cells produce a soluble factor capable of inducing osteoclastogenesis. Given that Cl66 cells express both cathepsin G and RANKL, this soluble factor is likely sRANKL. Thus, we would expect TPCK treatment to reduce the production sRANKL, which would reduce the concentration of sRANKL in the Cl66-conditioned medium and reduce osteoclastogenesis. As expected, TPCK abrogated the production of this soluble factor and reduced osteoclastogenesis, suggesting that cathepsin G is responsible for the generation of this soluble factor. Furthermore, Cl66 cells cocultured with RAW 264.7 cells also induced osteoclastogenesis that is reduced with TPCK treatment. Osteoclastogenesis is reduced but not eliminated because signaling via full-length, membrane-bound RANKL still occurs even with TPCK treatment. Thus, this is proof-in-principle that cathepsin G inhibition has the potential to reduce osteoclastogenesis and subsequent osteolysis *in vivo*. Based on these data, we subsequently sought to determine if inhibition of cathepsin G *in vivo* would reduce mammary tumor–induced osteolysis. TPCK treatment of mice significantly reduced osteolysis at the tumor-bone interface. In fact, TPCK-treated mice showed a 63% reduction in the bone destruction index. We did not observe a difference between TPCK-treated mice and control mice in terms of tumor growth or growth kinetics, suggesting that TPCK is not toxic to tumor cells and is not inducing apoptosis. In addition, our *in vitro* data suggest that

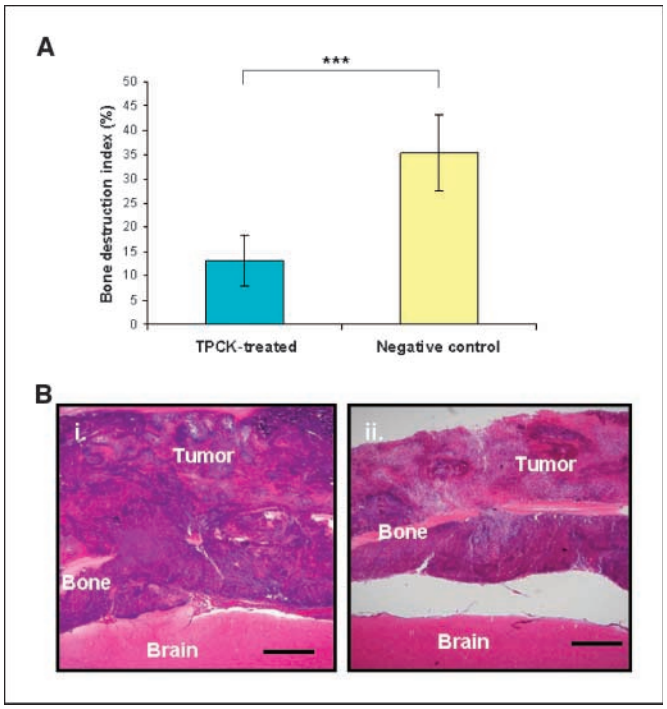

Figure 6. Inhibition of cathepsin G *in vivo* reduces osteolysis. *A,* TPCK treatment significantly reduced mammary tumor–induced osteolysis *in vivo* compared with DMSO-treated mice (*negative control*). *Bars,* SD. ***, $P < 0.001$ *B, i,* H&E-stained section of the tumor-bone interface from DMSO-treated mouse (negative control) showing significant osteolysis. *ii,* H&E-stained section of the tumor-bone interface from TPCK-treated mouse showing significantly reduced osteolysis. *Bar,* 2 mm.

TPCK is not toxic to osteoclasts. Thus, the mechanism by which TPCK inhibits osteolysis is likely via interruption of signaling between tumor cells and the bone microenvironment, and our data suggest that the pathway that is interrupted is the generation of sRANKL.

This reduction in osteolysis shows the central role that cathepsin G plays in mammary tumor–induced osteolysis *in vivo*. TPCK is a potent inhibitor of cathepsin G but is not specific to only cathepsin G (8). TPCK is also capable of inhibiting chymotrypsin, papain, bromelain, and ficin (7). Although TPCK is not specific for cathepsin G, given its ability to potently inhibit cathepsin G, taken with the lack of toxicity to tumor cells shown by no observable difference in tumor growth or growth kinetics, the lack of toxicity to osteoclasts as shown *in vitro* by treatment of RAW 264.7 cells with both TPCK and sRANKL, and the proposed mechanism by which inhibition of cathepsin G would reduce sRANKL and specifically decrease osteolysis, we believe that inhibition with TPCK adequately shows the role of cathepsin G in mammary tumor–induced osteolysis.

In conclusion, this study shows that cathepsin G plays an important role in mammary tumor–induced osteolytic lesions by contributing to the vicious cycle. It is significantly up-regulated at the tumor-bone interface and is capable of generating sRANKL, which potentially enhances osteoclast activation and osteolysis. We have also shown that inhibition of cathepsin G *in vitro* and *in vivo* reduces osteoclastogenesis and subsequent osteolysis. Thus, we have shown a central role for cathepsin G in the establishment of mammary tumor–induced osteolytic lesions. Further studies are needed to reveal the potential subsequent roles of cathepsin G, in addition to generation of soluble RANKL, in the bone tumor microenvironment. This study reveals cathepsin G as an appealing therapeutic target in mammary tumor–induced osteolysis.

Disclosure of Potential Conflicts of Interest

No potential conflicts of interest were disclosed.

Acknowledgments

Received 10/18/2007; revised 3/10/2008; accepted 5/19/2008.

Grant support: Grant CA72781 and Cancer Center Support Grant P30CA036727 from the NIH (R.K. Singh), Nebraska Department of Health and Human Services, Nebraska Research initiative (R.K. Singh), and the Howard Hughes Medical Institute Research Training Fellowship (T.J. Wilson).

The costs of publication of this article were defrayed in part by the payment of page charges. This article must therefore be hereby marked *advertisement* in accordance with 18 U.S.C. Section 1734 solely to indicate this fact.

We thank Michelle Varney for careful review and critique of the manuscript.

References

1. Jemal A, Siegel R, Ward E, Murray T, Xu J, Thun MJ. Cancer statistics, 2007. CA Cancer J Clin 2007;57:43–66.
2. Mundy GR. Metastasis to bone: causes, consequences and therapeutic opportunities. Nat Rev Cancer 2002;2:584–93.
3. Kajita M, Itoh Y, Chiba T, et al. Membrane-type 1 matrix metalloproteinase cleaves CD44 and promotes cell migration. J Cell Biol 2001;153:893–904.
4. Eliceiri BP, Cheresh DA. Role of α_v integrins during angiogenesis. Cancer J 2000;6 Suppl 3:S245–9.
5. Deryugina EI, Ratnikov BI, Postnova TI, Rozanov DV, Strongin AY. Processing of integrin α_v subunit by membrane type 1 matrix metalloproteinase stimulates migration of breast carcinoma cells on vitronectin and enhances tyrosine phosphorylation of focal adhesion kinase. J Biol Chem 2002;277:9749–56.
6. Lynch CC, Hikosaka A, Acuff HB, et al. MMP-7 promotes prostate cancer-induced osteolysis via the solubilization of RANKL. Cancer Cell 2005;7:485–96.
7. Overall CM, Blobel CP. In search of partners: linking extracellular proteases to substrates. Nat Rev Mol Cell Biol 2007;8:245–57.
8. Selak MA, Chignard M, Smith JB. Cathepsin G is a strong platelet agonist released by neutrophils. Biochem J 1988;251:293–9.
9. Yu Q, Stamenkovic I. Cell surface-localized matrix metalloproteinase-9 proteolytically activates TGF-β and promotes tumor invasion and angiogenesis. Genes Dev 2000;14:163–76.
10. Ishikawa T, Kamiyama M, Tani-Ishii N, et al. Inhibition of osteoclast differentiation and bone resorption by cathepsin K antisense oligonucleotides. Mol Carcinog 2001;32:84–91.
11. Nemeth JA, Yousif R, Herzog M, et al. Matrix metalloproteinase activity, bone matrix turnover, and tumor cell proliferation in prostate cancer bone metastasis. J Natl Cancer Inst 2002;94:17–25.
12. Ishibashi O, Niwa S, Kadoyama K, Inui T. MMP-9 antisense oligodeoxynucleotide exerts an inhibitory effect on osteoclastic bone resorption by suppressing cell migration. Life Sci 2006;79:1657–60.
13. Jimi E, Aoki K, Saito H, et al. Selective inhibition of NF-κB blocks osteoclastogenesis and prevents inflammatory bone destruction *in vivo*. Nat Med 2004;10:617–24.
14. Ohshiba T, Miyaura C, Inada M, Ito A. Role of RANKL-induced osteoclast formation and MMP-dependent matrix degradation in bone destruction by breast cancer metastasis. Br J Cancer 2003;88:1318–26.
15. Yasuda H, Shima N, Nakagawa N, et al. Osteoclast differentiation factor is a ligand for osteoprotegerin/osteoclastogenesis-inhibitory factor and is identical to TRANCE/RANKL. Proc Natl Acad Sci U S A 1998;95:3597–602.
16. Lacey DL, Timms E, Tan HL, et al. Osteoprotegerin ligand is a cytokine that regulates osteoclast differentiation and activation. Cell 1998;93:165–76.
17. Fujisaki K, Tanabe N, Suzuki N, et al. Receptor activator of NF-κB ligand induces the expression of carbonic anhydrase II, cathepsin K, and matrix metalloproteinase-9 in osteoclast precursor RAW264.7 cells. Life Sci 2007;80:1311–8.
18. Chesneau V, Becherer JD, Zheng Y, Erdjument-Bromage H, Tempst P, Blobel CP. Catalytic properties of ADAM19. J Biol Chem 2003;278:22331–40.
19. Schlondorff J, Lum L, Blobel CP. Biochemical and pharmacologic criteria define two shedding activities for TRANCE/OPGL that are distinct from the tumor necrosis factor α convertase. J Biol Chem 2001;276:14665–74.
20. Szekanecz Z, Koch AE. Macrophages and their products in rheumatoid arthritis. Curr Opin Rheumatol 2007;19:289–95.
21. Chavan V, Patil N, Karnik ND. Study of leukocytic hydrolytic enzymes in patients with acute stage of coronary heart disease. Indian J Med Sci 2007;61:73–82.
22. Komine K, Kuroishi T, Ozawa A, et al. Cleaved inflammatory lactoferrin peptides in parotid saliva of periodontitis patients. Mol Immunol 2007;44:1498–508.
23. Shimoda N, Fukazawa N, Nonomura K, Fairchild RL. Cathepsin g is required for sustained inflammation and tissue injury after reperfusion of ischemic kidneys. Am J Pathol 2007;170:930–40.
24. Campbell EJ, Owen CA. The sulfate groups of chondroitin sulfate- and heparan sulfate-containing proteoglycans in neutrophil plasma membranes are novel binding sites for human leukocyte elastase and cathepsin G. J Biol Chem 2007;282:14645–54.

Kalyan C. Nannuru

3828 Jones Street # 302, Omaha, NE 68105

402-960-5857 (Mobile), knannuru@unmc.edu, kcnannuru@gmail.com

PROFILE:

Cancer and Molecular biologist with a degree in doctor of veterinary medicine.

- Successful bench scientist with a strong publication record
- Extensive expertise in various molecular biology, cell biology, biochemical techniques, and animal tumor studies.
- Strong knowledge in statistical analysis with outstanding laboratory management skills
- Excellent communication and writing skills developed by participating in several national and local meetings, and by writing a number of scientific papers, abstracts and grants

RESEARCH/TECHNICAL SKILLS:

Animal work: Expertise in working with mouse model in breast cancer research including tumor implantation, tumor growth measurement, use of *in vivo* imaging technology (IVIS system) to monitor tumor progression, *In vivo* targeting of molecules with oligonucleotides or chemical inhibitors, processing of mice and collecting tissues for analysis. Hands on experience in bone targeting polymer studies and familiar with small animal CT scan, bone density scan procedures and working with KO mice

Molecular biology and biochemical techniques: Molecular cloning techniques, construction of conditional expression systems (tet-on and tet off), plasmid and oligonucleotide transfection of mammalian cells, shRNA, RNAi viral vector delivery into mammalian cells, PCR, Real Time-PCR, Western Blotting, ELISA Protease activity assays and zymograms, extensive experience in tissue analysis by Immunohistochemistry and Immnuoflurescence and Special tissue and cell staining procedures (TRAP, TUNEL) constructing and screening of Genomic expression library, Automated DNA sequencing, Genome sequence analysis, , Nested Deletion technique, RT-PCR, Cloning, Southern and Western Blotting Nucleic Acid and protein extraction, PAGE, PFGE, Primers and probe designing.

Cell culture work: Adequate experience in isolating and culturing mouse and human tumor cell lines and cells of bone microenvironment (Osteoblasts, Osteoclasts and stromal cells). Expertise in cell based assays including MTT cell proliferation assay, Cell invasion, migration and chemotaxis assays and Nitrate assays.

Software skills: Data handling techniques for qPCR and microarrays, Sigmaplot, SPSS, SAS, Vector NTi and GCG genetic analysis programs and well acquainted with MS office.

RESEARCH AND PROFESSIONAL EXPERIENCE:

PhD: Principal investigator: Dr. Rakesh K. Singh

Project title: *Molecular mechanisms of mammary tumor induced osteolysis in breast cancer bone metastasis.* Osteolytic bone metastasis in breast cancer is regulated by complex interactions of the tumor cells and bone microenvironment, which are mediated by specific molecules. Our work is focused on elucidating the role of RANKL, MMP13 and CXCR2 in breast cancer progression and osteolytic bone metastasis. We identified upregulation of RANKL and MMP13 at tumor-bone interface. My work has shown the significance of soluble RANKL generation at tumor-bone interface during osteolytic bone metastasis.

MS: Principal investigator: Dr. Roman R. Ganta

Project title: *Identification of immunodominant genes in Ehrlichia chaffeensis from a genomic expression library*. Human Monocytic Ehrlichiosis caused by a gram negative rickettsial organism *Ehrlichia chaffeensis*. My work is focused on identifying immunodominant genes of *Ehrlichia chaffeensis* from a genomic expression library screening. A putative 157 kDa protein was identified as a strong immunoreactive gene.

EDUCATION:

University of Nebraska Medical Center, Omaha, NE, Department of Pathology and Microbiology, **Ph.D in Cancer Research**, 2006-present

Kansas State University, Manhattan, KS, Department of Diagnostic Medicine and Pathobiology, **MS**, 2003-2005

Acharya N.G. Ranga Agricultural University, College of Veterinary Sciences, Titupati, INDIA**, Doctor of Veterinary Medicine,** 1996-2002

AWARDS & HONORS:

2009-	Received **2009 Norman and Bernice Harris Award for research excellence in Cancer.**
2008-	Received **Department of Defense (DOD) Predoctoral fellowship** under Breast Cancer Research Program
2008-	Received **American Association of Cancer Research-Aflac Scholar-in-training award**
2008-	Selected for **2008 International Student forum** for an oral presentation in Omaha, NE.
2007- 2010-	Received **University of Nebraska Medical Center graduate student fellowship**.
2007 -	Graduate College Cash Award for **best poster presentation**.

2007 - **First Place in Poster presentation award** – UNMC Awards 2007
2007 - Pathology and Microbiology cash award **for best research poster presentation**
2007 - **Third prize** winner at **38th Midwest Student Biomedical Research Forum**, Omaha, NE.
2007- Selected for **2007 International Student forum** for an oral presentation in **Tokyo**, **Japan**.
2006 - Selected for **2006 International Student forum** for an oral presentation in **Beijing**, **China**
2005 - Elected to Honor Society of Veterinary Medicine **Phi Zeta Sigma** Chapter
2004 - **American Society of Microbiology Corporate Student travel Grant** to attend 104th ASM General Meeting.
2004 - Elected for the Honor Society " **Phi Kappa Phi**" Kansas State University Chapter for academic excellence.
2003-2005 - Graduate Research Assistantship for MS, Kansas State University, Manhattan, KS
2002 - Clinical Internship Stipend at College of Veterinary Science, Tirupathi, India.
2002 - Secured College Second position in B.V.Sc&A.H (D.V.M) at College of Veterinary Science, Tirupathi, India.
2001 - College of Veterinary Science research grant for Earn While You Learn Poultry Project, Tirupathi, India.

PEER- REVIEWED PUBLICATIONS:

1. **Nannuru KC**, Futakuchi M, Sadanandam A, Wilson TJ, Varney ML, Myers KJ, et al. Enhanced expression and shedding of receptor activator of NF-kappaB ligand during tumor-bone interaction potentiates mammary tumor-induced osteolysis. *Clin Exp Metastasis 2009 DOI: 10.1007/s10585-009-9279-2, 2009.*
2. **Nannuru, KC,** Futakuchi, M, Varney, M.L, Vincent, TM, Marcusson, EG, and Singh RK. MMP13 regulates mammary tumor induced osteolysis by activating MMP9 and TGF β at Tumor-Bone interface. *(Under Revision, Cancer Res 2009).*
3. Wilson TJ, **Nannuru KC**, Singh RK. Cathepsin G-mediated activation of pro-matrix metalloproteinase 9 at the tumor-bone interface promotes transforming growth factor-beta signaling and bone destruction. *Mol Cancer Res 2009;7:1224-33*.
4. Wilson TJ, **Nannuru KC**, Futakuchi M, Singh RK. Cathepsin G-mediated enhanced TGF-beta signaling promotes angiogenesis via upregulation of VEGF and MCP-1. *Cancer Lett 2009*.
5. Singh S, **Nannuru KC**, Sadanandam A, Varney ML, Singh RK. CXCR1 and CXCR2 enhance human melanoma tumourigenesis, growth and invasion. *Br J Cancer 2009;May 19;100:1638-46*.
6. Wilson TJ, **Nannuru KC**, Singh RK. Cathepsin G recruits osteoclast precursors via proteolytic activation of protease-activated receptor-1. *Cancer Res 2009;69:3188-95*.
7. Futakuchi M, **Nannuru KC**, Varney ML, Sadanandam A, Nakao K, Asai K, et al. TGF-beta signaling at the tumor-bone interface promotes mammary tumor growth and osteoclast activation. *Cancer Sci 2009; 100:71-81*.
8. Singh S, Sadanandam A, **Nannuru KC**, Varney ML, Mayer-Ezell R, Bond R, et al. Small-molecule antagonists for CXCR2 and CXCR1 inhibit human melanoma growth by decreasing tumor cell proliferation, survival, and angiogenesis. *Clin Cancer Res 2009;15:2380-6.*
9. Singh S, Sadanandam A, Varney ML, **Nannuru KC**, Singh RK. Small interfering RNA-mediated CXCR1 or CXCR2 knock-down inhibits melanoma tumor growth and invasion. *Int J Cancer 2009*.
10. Wilson TJ, **Nannuru KC**, Futakuchi M, Sadanandam A, Singh RK. Cathepsin G enhances mammary tumor-induced osteolysis by generating soluble receptor activator of nuclear factor-kappaB ligand. *Cancer Res 2008;68:5803-11*.
11. **Nannuru KC**, Varney ML, and Singh RK. CXCR2 expression in mammary tumor cells promotes metastasis to lung and osteolysis during bone metastasis. (*Manuscript under preparation*)

SEQUENCES SUBMITTED TO NCBI:

Nannuru, K.C. and Ganta, R.R. *Ehrlichia chaffeensis* immunogenic genes identified from a genomic expression library

a. **DQ066453 6289 bp DNA,** *E.chaffeensis* Complete cds of pOMP, DNA polymerase β subunit genes, pseudogene, ribonuclease D, transcriptional activator protein and partial cds of phosporibosylamine glycine ligase pseudo gene.
b. **DQ066454 5314 bp DNA,** Ehrlichia chaffeensis p157 gene, partial cds.

RESEARCH TALKS AND POSTER PRESENTATIONS:

- American Association for Cancer Research (**AACR**) Annual meeting. 2007, 2008 and 2009
- Midwest Student Biomedical Research Forum (**MSBRF**), 2007, 2008 and 2009
- Graduate Student Research Seminar Series. Dept. of Pathology and Microbiology at UNMC. 2006, 2007 and 2008
- International Student Forum, 2006 (Beijing, China), 2007 (Tokyo, Japan) and 2008 (Omaha, NE)
- Breast Cancer Training Program, Eppley Cancer Institute at UNMC, 2007
- 104th American Society for Microbiology General Meeting, 2004
- Annual Graduate Student Council Research Forum, Kansas State University, 2004 and 2005
- Phi Zeta Research Day, College of Veterinary Medicine, Kansas State University, 2004 and 2005

GRANT EXPERIENCE:

- Received **Department of Defense (DOD) Breast Cancer Research predoctoral fellowship** for 3 years
- Received **UNMC graduate studies fellowship** 2006 to 2010.

LEADERSHIP/ ACADEMIC MEMBERSHIPS:

- Associate member of **American Association of Cancer Research (AACR)**
- **UNMC Student Senate,** 2-term Senator – 2007 and 2008
- Member of **Veterinary Council of India** as a Veterinary Doctor